PHYSICAL REVIEW D **93,** 124016 (2016)

Spectral decomposition of black-hole perturbations on hyperboloidal slices

Marcus Ansorg and Rodrigo Panosso Macedo
Theoretisch-Physikalisches Institut, Friedrich-Schiller-Universität Jena, Max-Wien-Platz 1, D-07743 Jena, Germany
(Received 6 April 2016; published 7 June 2016)

In this paper, we present a spectral decomposition of solutions to relativistic wave equations described on horizon-penetrating hyperboloidal slices within a given Schwarzschild-black-hole background. The wave equation in question is Laplace transformed, which leads to a spatial differential equation with a complex parameter. For initial data which are analytic with respect to a compactified spatial coordinate, this equation is treated with the help of the MATHEMATICA package in terms of a sophisticated Taylor series analysis. Thereby, all ingredients of the desired spectral decomposition arise explicitly to arbitrarily prescribed accuracy, including quasinormal modes and quasinormal mode amplitudes as well as the jump of the Laplace transform along the branch cut. Finally, all contributions are put together to obtain, via the inverse Laplace transformation, the spectral decomposition in question. The paper explains extensively this procedure and includes detailed discussions of relevant aspects, such as the definition of quasinormal modes and the question regarding the contribution of infinity frequency modes to the early time response of the black hole.

DOI: 10.1103/PhysRevD.93.124016

I. INTRODUCTION

Since the advent of general relativity, studies within the linear regime of Einsteins's equations have played a crucial role in understanding important aspects of both mathematical and physical sides of the theory. In the particular case of black-hole perturbation theory, the work by Regge and Wheeler [1] usually marks the birth of the field. Their analysis of a special class of perturbations of the Schwarzschild spacetime was later generalized by Zerilli [2,3]. Still in the context of the Schwarzschild spacetime, Bardeen and Press [4] used the Newman-Penrose formalism [5] to derive the equations describing the propagation of scalar, electromagnetic and gravitational wave perturbations within the aforementioned background. This approach is the same as the one that guided Teukolsky towards the derivation of his equation, which takes the Kerr solution as the background spacetime [6].

First observed by Vishveshwara [7], the time evolution of the perturbing field shows, after an initial dynamics, an intermediate phase dominated by exponentially damped oscillations, the so-called "quasinormal modes" (QNMs). The remarkable feature is that the oscillation and decay time scales depend solely on the black-hole parameters, which allows one to infer essential properties of the black hole in the gravitational wave signal [8] and to determine whether the object is a black hole or something else [9,10]. For the late time evolution, Price showed that the dynamics is characterized by a power law decay, also referred to as "tail decay" [11].

A complete revision of the literature related to this field is a task that goes beyond the scope of this work. Instead of overwhelming the reader with all the developments that followed the seminal works mentioned previously, we would rather point out Chadrasekhar's book [12] that reviews the state-of-art developments during the 1980s and elucidates the connections between different formalisms. Also worth mentioning are Refs. [13] and [14], the two reviews that appeared in the late 1990s. Finally, Berti, Cardoso and Starinets [15] summarized the more recent development on black-hole perturbation theory. Apart from a very interesting and useful chronological "roadmap" in terms of papers considered as milestones, the results presented in [15] range from astrophysical scenarios (with insights into the numerical simulations and the efforts to the detection of gravitational waves), passing by applications in gauge-gravity duality theories, up to some recent developments on quantum black holes. Among the many important milestones listed in [15], we mention here Leaver's work [16–18], which provides one of the most accurate methods to compute the QNMs.

Note however, that in the great majority of these works, QNMs are defined in a phenomenological way motivated by a comparison with the analysis of normal modes (see, for example, [19]).

A formal definition of the QNMs is presented in the second chapter of Ref. [13]. It starts out with the description of normal modes as the real eigenvalues ω_n of an appropriate differential operator. This operator acts on a corresponding Hilbert-space whose measure characterizing the inner product, arises through the requirement that the operator be self-adjoint. The eigenvalues can then be used along with the associated eigenvectors $\phi_n(x^k)$ to build up the solutions V of a specific nondissipative wave equation,[1]

[1]In this paper, time in the wave equations is denoted by τ, whereas x^k ($k = 1\ldots3$) stands for the collection of relevant spatial coordinates.

$$V(\tau, x^k) = \sum_{n=0}^{\infty} \eta_n e^{i\omega_n \tau} \phi_n(x^k). \quad (1)$$

Of course, this only works if the self-adjoint operator in question has a pure point spectrum $\sigma_p = \{\omega_n\}_{n=0}^{\infty}$. More generally, if in addition a continuous spectrum σ_c is present, then the superposition needs to include improper eigenvalues and eigenvectors:

$$V(\tau, x^k) = \sum_{n=0}^{\infty} \eta_n e^{i\omega_n \tau} \phi_n(x^k) + \int_{\omega \in \sigma_c} \eta(\omega) e^{i\omega\tau} \phi(\omega; x^k) d\omega. \quad (2)$$

The computation of the corresponding amplitudes, η_n and $\eta(\omega)|_{\omega\in\sigma_c}$, amounts to projecting the initial data onto the complete orthonormal system of (proper and improper) eigenfunctions in terms of the inner product.

As expressed in the review [13], it would be clearly desirable to take this formulation to the realm of linear black-hole perturbations, that is, to write the solutions of initial value problems associated with linear dissipative wave equations in a given black-hole background-metric as a similar superposition, with the quasinormal modes being defined as the eigenvalues of an appropriate operator. However, the very definition of the QNMs, as pursued in [13], follows a different route. Through a Laplace transform applied to the wave equation in question, a spatial differential equation arises with an inhomogeneity formed by the initial data. The QNMs are then defined as the zeros of the corresponding Wronskian determinant, formed by specifically normalized solutions of the associated homogeneous equation. This definition is a perfectly working characterization of QNMs in many situations. However, in the context of linear perturbations in asymptotically flat black-hole spacetimes, it appears that a corresponding direct computation poses substantial technical difficulties. In this paper (Sec. IV D), we provide a detailed discussion of this matter.

Until now there is no strict mathematical derivation of a spectral decomposition formula (2) for linear waves around asymptotically flat black holes. Nevertheless, in special cases it was shown [20] that the late time behavior of the solutions can be approximated in finite parts of the space by a finite sum of the form (1). In [21], it was demonstrated that for a wave equation with so called spiked truncated dipole potential the decomposition (1) can be constructed; particularly the amplitudes η_n were determined explicitly. Moreover, in several papers [18,22–24], so-called "quasinormal excitation factors" are discussed which are determined through the behavior of ϕ_n at the two boundaries describing spatial infinity and the event horizon. They serve for the determination of quasinormal excitation coefficients which are equivalent to the expressions $\eta_n\phi_n$. Rigorous mathematical results including integral representations have been obtained in the case of Cauchy problems for the massive Dirac equation as well as for the Teukolsky-equation in the nonextreme Kerr-Newman geometry outside the event horizon; see e.g. [25–29].

In this paper, we demonstrate that a superposition of the form

$$V(\tau,x^k)=\sum_{n=0}^{\infty}\eta_n e^{s_n\tau}\phi_n(x^k)+\int_{-\infty}^{0}\eta(s)e^{s\tau}\phi(x^k;s)ds \quad (3)$$

can be found for solutions of initial value problems of linear wave equations in the Schwarzschild spacetime, provided that the initial data are analytical in terms of a compactified coordinate in an appropriate hyperboloidal slice to be specified in Sec. II A. The amplitudes η_n and $\eta(s)$ are fixed solely by the initial data, whereas the quasinormal modes s_n as well as the functions $\phi_n(x^k)$ and $\phi(x^k;s)$ are characteristics of the particular wave equation being studied and hence independent of the initial data. We stress that (3) is meant to provide, in a strict sense, the entire solution for all coordinate times $\tau > \nu$ where ν is a mutual growth rate of the excitation coefficients $\eta_n\phi_n(x^k)$ and $\eta(s)\phi(x^k;s)$ to be defined in the sequel (see Secs. IV E and IV F).

Now, in order to describe the decay of a dissipative wave field, the QNMs s_n need to be complex valued with negative real part. Hence, an associated self-adjoint operator with spectrum $\sigma = \{s_n\}_{n=0}^{\infty} \cup (-\infty, 0)$ cannot be identified. Consequently, it is not simply possible to establish η_n and $\eta(s)$ by some orthogonal projection of the initial data onto the functions $\phi_n(x^k)$ and $\phi(x^k;s)$. Nevertheless, in this paper, we develop highly accurate numerical means, based on a detailed Taylor series analysis which is established within the MATHEMATICA environment, through which all ingredients of (3) are determined:

(1) The QNMs s_n are computed through an efficient procedure which can be considered as an extension of Leaver's method of continued fractions [16,17].
(2) The functions $\phi_n(x^k)$ and $\phi(x^k;s)$ are constructed from the wave equation under consideration (without the need to consider specific initial data).
(3) The amplitudes η_n and $\eta(s)$, being characteristics of the initial data, are obtained through an analysis that incorporates the initial data.

In addition, we provide strong evidence that the solutions $V(\tau, x^k)$ to initial value problems of wave equations in the Schwarzschild spacetime for analytical initial data as described above are indeed entirely given in terms of (3) for all coordinate times τ that exceed the growth rate ν of the excitation coefficients.

As mentioned above, we concentrate in this paper on a hyperboloidal formulation. However, typically the black hole perturbation theory is developed with the background metric described in terms of a coordinate system with slices of constant time extending between the bifurcation point $\mathcal{B}$

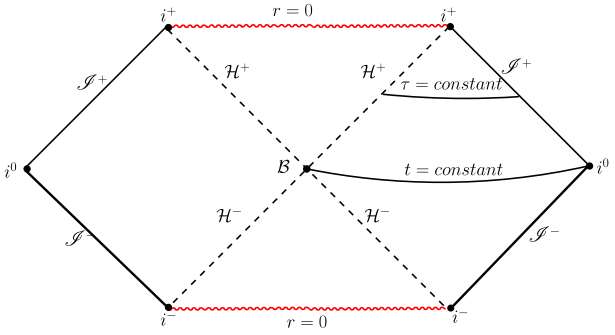

FIG. 1. Penrose-Carter conformal diagram for the extended Schwarzschild spacetime. Future and past event horizons are denoted by $\mathcal{H}^+$ and $\mathcal{H}^-$ respectively. Likewise, future and past null infinity are specified through $\mathcal{I}^+$ and $\mathcal{I}^-$ respectively. The bifurcation point $\mathcal{B}$ describes the mutual meeting point of the several horizons in this diagram. Also shown is a typical hyperboloidal slice $\tau=$ const extending smoothly through both $\mathcal{H}^+$ and $\mathcal{I}^+$, as well as a Cauchy slice $t=$ const extending from the bifurcation point $\mathcal{B}$ to spatial infinity i^0.

and spatial infinity i^0; see the Penrose-Carter conformal diagram in Fig. 1.

The most simple example is given by the Schwarzschild spacetime written in terms of the well known Schwarzschild-coordinates $\{t,r,\theta,\varphi\}$. In this context, apart from the data at the initial time slice, one needs to impose boundary conditions at $\mathcal{B}$ as well as at i^0 since the physical solution should contain only ingoing (outgoing) radiation at the horizon (spatial infinity). When treating the wave equation in terms of its Laplace transform, this framework leads to solutions of the spatial equation which grow exponentially near the boundaries. Note that the review [14] lists many difficulties for obtaining the desired representation (3), and the issue regarding the blow up of the solutions near the boundaries constitutes one of the main drawbacks.

To overcome these caveats, the author of [30] argues in favor of a coordinate system with time-constant surfaces extending between the future event horizon $\mathcal{H}$ and future null infinity $\mathcal{I}^+$, also known as hyperboloidal slices; see [31] for a review. The work [30] shows that this choice resolves the issues concerning the representation of the functions associated to the QNMs. The paper emphasizes the advantage of this framework in comparison with other methods and mentions that developing a black hole perturbation theory on hyperboloidal slices "may lead to efficient numerical codes in the frequency domain" [30]. The work does, however, not advance further in this direction. In this paper, we exploit the advantages of the formulation of linear wave equations in the Schwarzschild spacetime on hyperboloidal slices.

The paper is organized as follows. In Sec. II, we describe the coordinate transformation leading to the hyperboloidal slices in the Schwarzschild spacetime, and we introduce the Bardeen-Press equation that describes scalar, electromagnetic and gravitational perturbations propagating on this background. Section III is devoted to the Laplace transformation of the Bardeen-Press equation, thereby obtaining a characteristic spatial equation. Moreover, the inversion through the so-called "Bromwich integral" is discussed. This section also brings a comparison with the corresponding formulation of black-hole perturbation theory on Cauchy slices. In the comprehensive Sec. IV, we apply sophisticated Taylor series expansions in order to get the solutions of the spatial equations. This analysis provides us with the various ingredients of the spectral representation (3) of the solution which is then derived in Sec. V. Section VI brings a thorough discussion, including a comparison with a similar problem in Minkowski spacetime which can be treated explicitly. The Appendix comprises several sections in order to elaborate on certain aspects and issues that appear in the course of the text. Especially, the so-called algebraically special QNMs [32] are discussed. Note that we use units such that the speed of light as well as Newton's constant of gravity are unity, $c=G=1$.

II. BLACK-HOLE PERTURBATION WITHIN A HYPERBOLOIDAL FOLIATION

A. Hyperboloidal coordinates

Our starting point is a review of the hyperboloidal coordinates used for the spacetime foliation. Following [33,34], we write at first the Schwarzschild metric for a black hole with mass M in the horizon-penetrating ingoing Eddington-Finkelstein coordinates $\{v,r,\theta,\phi\}$ and introduce then the new coordinates (τ,σ) via

$$v=4M\left(\tau+\frac{1}{\sigma}-\log\sigma\right) \tag{4}$$

$$r=\frac{2M}{\sigma}. \tag{5}$$

As a result, we obtain the line element

$$ds^2=\frac{16M^2}{\sigma^2}\Big[-\sigma^2(1-\sigma)d\tau^2+(1+\sigma)d\sigma^2 + (1-2\sigma^2)d\tau d\sigma+\frac{1}{4}(d\theta^2+\sin^2\theta d\varphi)\Big]. \tag{6}$$

In the hyperboloidal coordinates $\{\tau,\sigma,\theta,\phi\}$, the horizon is given by $\sigma=1$, while $\mathcal{I}^+$ is fixed at $\sigma=0$.

B. Bardeen-Press equation

The equation describing the dynamics of a perturbation U in a background given by the Schwarzschild solution was derived[2] by Bardeen and Press [4]. The equation reads in our hyperboloidal coordinates $\{\tau,\sigma,\theta,\varphi\}$ [34]

[2]The equation is equivalent to the Teukolsky equation [6] with vanishing specific angular momentum parameter, $a=0$.

TABLE I. Perturbation field and spin-weight λ.

λ	U	$\sigma \to 0$
0	Φ	$\Phi = \mathcal{O}(\sigma)$
1	ϕ_0	$\phi_0 = \mathcal{O}(\sigma^3)$
−1	$\sigma^{-2}\phi_2$	$\phi_2 = \mathcal{O}(\sigma)$
2	Ψ_0	$\Psi_0 = \mathcal{O}(\sigma^5)$
−2	$\sigma^{-4}\Psi_4$	$\Psi_4 = \mathcal{O}(\sigma)$

$$
\begin{aligned}
&-(1+\sigma)U_{,\tau\tau} + (1-2\sigma^2)U_{,\tau\sigma} + (1-\sigma)\sigma^2 U_{,\sigma\sigma} \\
&\quad - \left(\frac{1+2\lambda}{\sigma} - \lambda\frac{2-\sigma}{1-\sigma}\right)U_{,\tau} - \sigma[\sigma + \lambda(2-\sigma)]U_{,\sigma} \\
&\quad + U_{,\theta\theta} + U_{,\theta}\cot\theta + \frac{1}{\sin^2\theta}(U_{,\varphi\varphi} + 2i\lambda\cos\theta U_{,\varphi}) \\
&\quad + \lambda(1 - \lambda\cot^2\theta)U = 0. \qquad (7)
\end{aligned}
$$

The field $U(\tau,\sigma,\theta,\varphi)$ has spin-weight λ. A scalar field Φ propagating on the background is described by $\lambda = 0$. If $\lambda = -1$ ($\lambda = +1$), $U(\tau,\sigma,\theta,\varphi)$ is closely related to the Newman-Penrose scalars [5] ϕ_2 (ϕ_0) describing outgoing (ingoing) electromagnetic waves. In the same way, gravitational waves are associated to Newman-Penrose scalars Ψ_4 (Ψ_0) with spin weight $\lambda = -2$ ($\lambda = +2$). Table I brings the relation between $U(\tau,\sigma,\theta,\varphi)$ and the different types of fields according to the corresponding spin λ. The table also shows the asymptotic behavior of such fields around $\mathcal{I}^+$ ($\sigma \to 0$) in accordance with the Peeling theorem [5].

Note that Eq. (7) is irregular at $\sigma = 0$ and $\sigma = 1$, i.e., at future null infinity and at the horizon, respectively. This property is a direct consequence of our hyperboloidal slicing. Taking into account the relation of $U(\tau,\sigma,\theta,\varphi)$ with the respective Newman-Penrose quantities and their asymptotic behavior as depicted in table I, one can introduce the regular field $\tilde{U}$

$$U(\tau,\sigma,\theta,\varphi) = \sigma^{1+2\lambda}\tilde{U}(\tau,\sigma,\theta,\varphi)$$

which removes the singular term going as σ^{-1} from (7). Moreover, as noted in [30], the singular term at $\sigma = 1$ is removed by the further re-scaling

$$U(\tau,\sigma,\theta,\varphi) = \sigma^{1+2\lambda}(1-\sigma)^{-\lambda}V(\tau,\sigma,\theta,\varphi). \qquad (8)$$

We expand the field $V(\tau,\sigma,\theta,\varphi)$ into the spin-weighted spherical harmonics ${}_\lambda Y_{\ell m}(\theta,\varphi)$ basis [35]

$$V(\tau,\sigma,\theta,\varphi) = \sum_{\ell=|\lambda|}^{\infty}\sum_{m=-\ell}^{\ell} V_{\ell m}(\tau,\sigma)\,{}_\lambda Y_{\ell m}(\theta,\varphi),$$

thus obtaining a specific wave equation for each mode $V_{\ell m}(\tau,\sigma)$[3]:

$$
\begin{aligned}
&-(1+\sigma)V_{,\tau\tau} + (1-2\sigma^2)V_{,\tau\sigma} + \sigma^2(1-\sigma)V_{,\sigma\sigma} \\
&\quad + \sigma[2 - 3\sigma + \lambda(2-\sigma)]V_{,\sigma} - [2\sigma - \lambda(1-\sigma)]V_{,\tau} \\
&\quad + [-\ell(\ell+1) - (\sigma-\lambda)(1+\lambda)]V = 0. \qquad (9)
\end{aligned}
$$

Given initial data $V_0(\sigma) = V(0,\sigma)$ and $\dot{V}_0(\sigma) = V_{,\tau}(0,\sigma)$, Eq. (9) is to be solved in the domain $(\tau,\sigma) \in [0,\tau_{\text{final}}] \times [0,1]$.

Note that the transition from the field U to V has not removed the degeneracies of the wave equation at the two boundaries $\sigma = 0$ and $\sigma = 1$. These degeneracies provide boundary conditions that guarantee that the characteristics of the wave equation always point outward the numerical domain and hence no further boundary conditions at the horizon nor at future null infinity $\mathcal{I}^+$ are allowed to be imposed. Consequently, equation (9) has to be solved as an initial value problem.

III. LAPLACE TRANSFORMATION

A. Definition

Given initial data $V_0(\sigma)$ and $\dot{V}_0(\sigma)$, we follow [13] and introduce the Laplace transformation

$$\hat{V}(\sigma;s) := \mathcal{L}[V(\tau,\sigma)](s) = \int_0^\infty e^{-s\tau}V(\tau,\sigma)d\tau. \qquad (10)$$

As the field V is strictly bounded for all times τ, it follows that $\hat{V}(\sigma;s)$ is complex-holomorphic in the right half-plane $\Re(s) > 0$ (see Fig. 2). Note that the following relation is a particular consequence of the fact that the wave-field $V(\tau,\sigma)$ is real[4]:

$$\hat{V}(\sigma;s^*) = [\hat{V}(\sigma;s)]^*. \qquad (11)$$

Applying now the Laplace transformation to both sides of the dynamical equation (9) and considering that

$$
\begin{aligned}
\mathcal{L}[V_{,\tau}(\tau,\sigma)](s) &= s\hat{V}(\sigma;s) - V_0(\sigma), \\
\mathcal{L}[V_{,\tau\tau}(\tau,\sigma)](s) &= s^2\hat{V}(\sigma;s) - sV_0(\sigma) - \dot{V}_0(\sigma),
\end{aligned}
$$

we obtain an inhomogeneous ordinary differential equation (referred to as "ODE" in the sequel)[5]

$$\mathbf{A}(s)\hat{V}(s) = B(s) \qquad (12)$$

with the second order differential operator given by

[3]For simplicity, we omit the indices ℓm in $V_{\ell m}(\tau,\sigma)$ from now on.

[4]Throughout this paper, we use an upper asterisk * to denote *complex conjugation*.

[5]For addressing the function $\hat{V}$ defined for $\sigma \in [0,1]$ (rather than a particular function value within that interval), we simply write $\hat{V}(s)$. The same applies to the right-hand side B.

$$\mathbf{A}(s)=\sigma^2(1-\sigma)\partial_{\sigma\sigma}+\{s(1-2\sigma^2)+\sigma[2-3\sigma+\lambda(2-\sigma)]\}\partial_\sigma - \{s^2(1+\sigma)+s[2\sigma+\lambda(\sigma-1)]+\ell(\ell+1) +(\sigma-\lambda)(\lambda+1)\}. \quad (13)$$

The degeneracies of the wave equation (9) (see discussion at the end of Sec. II B) implies that of the operator $\mathbf{A}(s)$ at the surfaces $\sigma=0$ and $\sigma=1$. The inhomogeneity $B(s)$ in (12) is given in terms of the initial data $V_0=V_0(\sigma)$ and $\dot{V}_0=\dot{V}_0(\sigma)$:

$$B(s)=(1-2\sigma^2)V_{0,\sigma}-(1+\sigma)\dot{V}_0 - [2\sigma-\lambda(1-\sigma)]V_0-s(1+\sigma)V_0. \quad (14)$$

B. Inversion

The solution of equation (12) with the help of a sophisticated Taylor series expansion will be depicted in Sec. IV. Once established $\hat{V}(\sigma;s)$ for values s on some vertical line in the right half-plane $\Re(s)>0$ (i.e. for $\Re(s)=\xi$ with some fixed $\xi>0$), we may write the solution of Eq. (9) in terms of the inverse Laplace transformation, also known as the Bromwich integral

$$V(\tau,\sigma)=\frac{1}{2\pi i}\int_{\Gamma_1}\hat{V}(\sigma;s)e^{s\tau}ds, \quad (15)$$

with the integration path (see Fig. 2)

$$\Gamma_1=\{s\in\mathbb{C}|s=\xi+i\chi,\xi>0,\chi\in(-\infty,+\infty)\}. \quad (16)$$

Note that (15) provides us with the solution $V(\tau,\sigma)$ only if $\tau>0$ (for $\tau<0$ the integral vanishes).

We remark that the formula (15) is the starting point for the spectral decomposition (3) which comes about through an appropriate deformation of the integration path (see Fig. 2) to be discussed in Sec. V.

C. Comparison with Cauchy foliation

We end this section with a brief discussion on some relations between the Laplace transformation performed in the context of hyperboloidal foliation and the corresponding formulation of perturbation theory in the original Schwarzschild coordinates.

Note that typically, perturbations on the Schwarzschild background are described by the Regge-Wheeler-Zerilli formalism, while here we focus on the Bardeen-Press-Teukolsky approach. Both formalisms are known to be equivalent and, in particular, the equations coincide for $\lambda=0$ (scalar perturbation). Therefore, along the paper, the discussion between the different foliations of the spacetime will always be made for the particular case $\lambda=0$. The conclusions, however, are general and should be valid also for $\lambda\neq 0$.

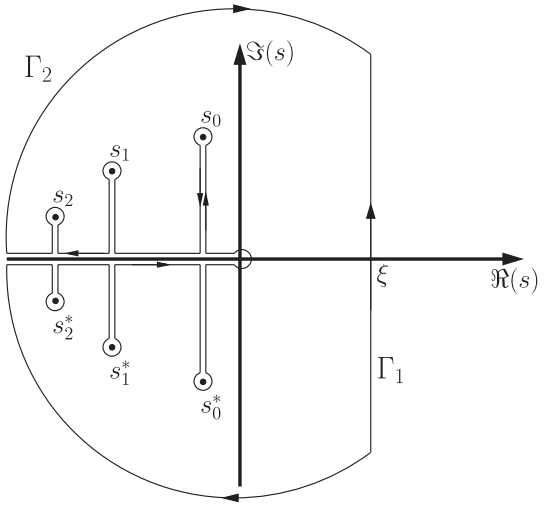

FIG. 2. Integration paths for the inverse Laplace transformation. The Bromwich integral (15) is evaluated along the line Γ_1 in the half-plane $\Re(s)>0$. In order to arrive at the spectral decomposition formula (3), it is essential to deform the integration path and to obtain the solution via integration along the curve Γ_2. The several ingredients, i.e. integration around the QNMs s_n, along the branch cut $\mathbb{R}^-$ as well as along infinitely extended circular sections, are discussed in detail in Sec. V.

Let us first introduce the dimensionless coordinates $x=r^*/(2M)$ and $\bar{t}=t/(2M)$ where r^* is the so-called tortoise coordinate. They are related to $\{\tau,\sigma\}$ via [cf. Eqs. (4) and (5)]

$$x=\frac{1}{\sigma}-\ln(\sigma)+\ln(1-\sigma), \quad (17)$$

$$\bar{t}=2\tau+\frac{1}{\sigma}-\ln[\sigma(1-\sigma)]. \quad (18)$$

The horizon is described by $x\to-\infty$ and spatial infinity is given by $x\to+\infty$. These points correspond to the bifurcation point $\mathcal{B}$ and i^0 in the Penrose diagram (see Fig. 1).

Then, Eq. (9) is equivalent to the well-known wave equation

$$-f_{,\bar{t}\bar{t}}+f_{,xx}-\mathcal{P}f=0, \quad (19)$$

with $f(\bar{t},x)=V(\tau(\bar{t},x),\sigma(x))$ and

$$\mathcal{P}=\left(1-\frac{2M}{r}\right)\left(\frac{2M}{r}\right)^2\left[\frac{2M}{r}+\ell(\ell+1)\right] =(1-\sigma)\sigma^2[\sigma+\ell(\ell+1)]. \quad (20)$$

Now, we apply the Laplace transformation

$$\hat{f}(x;\bar{s}):=\mathcal{L}[f(\bar{t},x)](\bar{s})=\int_0^\infty e^{-\bar{s}\bar{t}}f(\bar{t},x)d\bar{t}. \quad (21)$$

to Eq. (19) and obtain the equation

$$\hat{f}_{,xx} - [\bar{s}^2 + \mathcal{P}]\hat{f} = \dot{f}_0(x) + \bar{s} f_0(x), \tag{22}$$

where $f_0(x) = f(0,x)$ and $\dot{f}_0(x) = f_{,\bar{t}}(0,x)$ are the initial data and $\bar{s}$ the Laplace parameter in the Cauchy formulation.

Considering the homogeneous equations, we find the following relation between the Cauchy and the hyperboloidal formulation. Given a function $\Omega(s)$ that satisfies the ODE $\mathbf{A}(s)\Omega(s) = 0$ [cf. (12) and (13)]. Then the function

$$F(x(\sigma);\bar{s}) = 2e^{-\bar{s}/\sigma}\sigma^{\bar{s}}(1-\sigma)^{\bar{s}}\Omega(\sigma;2\bar{s}) \tag{23}$$

obeys the equation

$$F_{,xx} - [\bar{s}^2 + \mathcal{P}]F = 0 \tag{24}$$

where the Laplace parameter s (from our hyperboloidal foliation) is related to the Cauchy Laplace parameter $\bar{s}$ via

$$s = 2\bar{s}. \tag{25}$$

Note that (up to constants) the term

$$\Xi(\sigma;\bar{s}) = 2e^{-\bar{s}/\sigma}\sigma^{\bar{s}}(1-\sigma)^{\bar{s}} \tag{26}$$

corresponds exactly to the factor introduced by Leaver [16] accounting for the correct behavior of F at the boundaries $x \to \pm\infty$. Here, the relevant factor (26) is motivated by the term $e^{-\bar{s}\,\bar{t}(\tau,\sigma)}$ in (21), i.e., it follows directly from the hyperboloidal coordinates as a consequence of the fact that $\tau = \text{const}$ surfaces extend smoothly between the black horizon $\mathcal{H}^+$ and future null infinity $\mathcal{I}^+$.

IV. TAYLOR SERIES EXPANSIONS

A. Solutions to the homogeneous Laplace transformed equation and the asymptotics of their Taylor coefficients

Let us exclude, for the time being, nonpositive integer values of the Laplace parameter s, i.e. $s \notin \mathbb{Z}_0^-$.[6] We then start with the homogeneous Laplace transformed equation

$$\mathbf{A}(s)\phi(s) = 0, \qquad \phi(\sigma;s) \text{ analytic for } \sigma \in (0,1] \tag{27}$$

and expand $\phi(s)$ in terms of a Taylor series

$$\phi(\sigma;s) = \sum_{k=0}^{\infty} H_k(1-\sigma)^k. \tag{28}$$

With this ansatz, we follow Leaver [16] and concentrate, in a first step, on solutions which are analytic in a neighborhood about the horizon $\mathcal{H}$, i.e. at $\sigma = 1$. Inserting the ansatz (28) into (27), we obtain the following recurrence relation,

$$\alpha_k H_{k+1} + \beta_k H_k + \gamma_k H_{k-1} = 0, \tag{29}$$

with the coefficients:

$$\begin{aligned} \alpha_k &= (k+1)(k+1+s-\lambda), \\ -\beta_k &= 2(k+s)(k+1+s) + \ell(\ell+1) - \lambda^2 + 1, \\ \gamma_k &= (k+s)(k+s+\lambda). \end{aligned} \tag{30}$$

The coefficients H_k can now be obtained for $k \geq 1$ via

$$H_{k+1} = -\frac{1}{\alpha_k}(\beta_k H_k + \gamma_k H_{k-1}) = 0, \qquad H_0 \overset{!}{=} 1, \tag{31}$$

where we have chosen $H_0 = 1$ as convenient scaling condition. Note that for $k \geq 1$ we have $\alpha_k \neq 0$ as long as $s \notin \mathbb{Z}_0^-$; see (30). We study now the asymptotics of H_k for large indices $k \to \infty$.

The singular points of the ODE (27) are given by $\sigma = 0$, $\sigma = 1$, and $\sigma = \infty$. Consequently, we expect the series (28) to be convergent within the unit circle

$$\mathbf{C} = \{\sigma \in \mathbb{C} : |1-\sigma| < 1\}, \tag{32}$$

with analyticity breaking down at $\sigma = 0$, as this represents an essentially singular point of the ODE. We may therefore conclude that the domain of convergence of (28) does not exceed the unit circle $\mathbf{C}$, implying that

$$\lim_{k\to\infty}\left|\frac{H_{k+1}}{H_k}\right| = 1. \tag{33}$$

An asymptotic estimate was found by Leaver [16]

$$\frac{H_{k+1}}{H_k} = 1 \pm \sqrt{\frac{s}{k}} + \frac{\lambda + s - \frac{3}{4}}{k} + \mathcal{O}(k^{-3/2}),$$

from which we derive:

$$\log H_{k+1} = \log H_k \pm \sqrt{\frac{s}{k}} + \frac{\lambda + \frac{s}{2} - \frac{3}{4}}{k} + \mathcal{O}(k^{-3/2}).$$

Applying this formula successively from some $k = k_0$ on, we obtain the asymptotic formula

$$\begin{aligned} \log H_{k+1} &= \pm\sqrt{s}\sum_{j=k_0}^{k}\frac{1}{\sqrt{j}} + \left(\lambda + \frac{s}{2} - \frac{3}{4}\right)\sum_{j=k_0}^{k}\frac{1}{j} + \mathcal{O}(1) \\ &= \pm\sqrt{s}[H_k^{(1/2)} - H_{k_0-1}^{(1/2)}] \\ &\quad + \left(\lambda + \frac{s}{2} - \frac{3}{4}\right)[H_k^{(1)} - H_{k_0-1}^{(1)}] + \mathcal{O}(1) \end{aligned}$$

[6] In Appendix C, we extend our results to negative integer values s.

with

$$H_k^{(\nu)} = \sum_{j=1}^{k} \frac{1}{j^\nu} \tag{34}$$

being *generalized harmonic numbers*. Now these numbers possess the following asymptotics:

$$H_k^{(1/2)} = 2\sqrt{k} + \mathcal{O}(1), \qquad H_k^{(1)} = \log k + \mathcal{O}(1), \tag{35}$$

from which it follows that for sufficiently large k:

$$H_k = k^\zeta (A_k^+ e^{\kappa\sqrt{k}} + A_k^- e^{-\kappa\sqrt{k}}), \tag{36}$$

with

$$\kappa = 2\sqrt{s}, \qquad \Re(\kappa) > 0, \qquad \zeta = \lambda + \frac{s}{2} - \frac{3}{4}, \tag{37}$$

and where the coefficients $A_k^\pm$ tend to a finite value as $k \to \infty$, to be denoted by $A_\infty^\pm$. Again, this result corresponds to the findings by Leaver [17].

If we now investigate the behavior of the corresponding solution ϕ of (27) we observe that, for $\Re(s) > 0$, it possesses an essential singularity at $\sigma = 0$, somewhat similar to the function $e^{s/\sigma}$.[7] A more sophisticated analysis (to be conducted in Appendix B) reveals that

$$\Phi(\sigma; s) \coloneqq \sigma^{s+2\lambda} e^{-s/\sigma} \phi(\sigma; s) \tag{38}$$

is, for $\Re(s) > 0$, analytic at any $\sigma \in (0, 1]$ and still C^∞ at $\sigma = 0$. However, just as the function $e^{s/\sigma}$, the behavior of ϕ changes, when moving into the left half-plane $\Re(s) < 0$, as here ϕ becomes C^∞ for all $\sigma \in [0, 1]$. This fact has the interesting consequence that for $\Re(s) < 0$ the solutions $\phi(s)$ of (27) can be taken as regular C^∞ initial data,

$$V(0, \sigma) = \Re[\phi(\sigma, s)], \qquad V_{,\tau}(0, \sigma) = \Re[s\phi(\sigma, s)] \tag{39}$$

which imply the regular C^∞-solution

$$V(\tau, \sigma) = \Re[\phi(\sigma, s) e^{s\tau}] \tag{40}$$

to our wave equation (9).

We observe that the solution (40) behaves like a purely quasinormal ringing, with damping $\Re(s)$ and frequency $\Im(s)$. Figure 3 exemplifies this behavior by showing the time evolution (obtained through the algorithm presented in [34]) for this type of initial data. In particular, in the case $\lambda = \ell = 0$ the values $s = -1 + \pi i$ and $s = -2 + 2\pi i$ have been taken. However, these arbitrarily chosen s values in the left plane are to be distinguished from the QNMs to be discussed in Sec. IV D.[8]

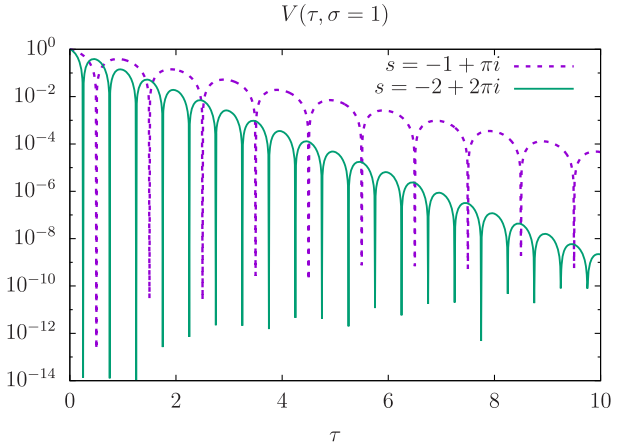

FIG. 3. Time evolution for initial data given by (39). For arbitrarily prescribed s values with $\Re(s) < 0$, the evolution shows exponentially damped oscillations [cf. (40)]. Here, the examples are obtained for $s = -1 + \pi i$ and $s = -2 + 2\pi i$ in the case $\lambda = \ell = 0$. The field is measured at $\sigma = 1$.

Let us now turn to a specific second solution $\psi(s)$ obeying the homogeneous Laplace transformed equation

$$\mathbf{A}(s)\psi(s) = 0. \tag{41}$$

We describe this solution by a sequence $\{I_k\}_{k=-\infty}^{\infty}$ of coefficients satisfying

$$\alpha_k I_{k+1} + \beta_k I_k + \gamma_k I_{k-1} = 0, \qquad \lim_{k\to\infty} I_k e^{\kappa\sqrt{k}} k^{-\zeta} = 1. \tag{42}$$

Here we have chosen the asymptotics (36) [which holds for any solution to the homogeneous recursion relation (29)] with $A_\infty^+ = 0$ and, moreover, $A_\infty^- = 1$ as convenient scaling condition.

Let us discuss the corresponding solution ψ in some detail. The sequence $\{I_k\}_{-\infty}^{\infty}$, which is uniquely defined by (42), does not provide us with a decent Laurent representation of ψ. An analysis of the asymptotics of I_k as $k \to -\infty$, performed along the same lines as the above investigation in the case $k \to +\infty$, reveals that

$$\lim_{m\to\infty} (e^{-2\sqrt{-sm}} m^{-\zeta} I_{-m}) = B_\infty^+ \quad \text{with} \quad |B_\infty^+| < \infty. \tag{43}$$

Here, the square root in the exponent is again to be taken such that its real part is positive. If we now consider principal part $\{I_k\}_{-\infty}^{-1}$ and secondary part $\{I_k\}_0^{\infty}$ separately,

[7] Indeed, it can be shown that the Taylor series (28) of $e^{s/\sigma}$ possesses the dominant asymptotics $H_k = e^{2\sqrt{sk}} k^{-3/4} A_k^+$ with $A_k^+ \to A_\infty^+(s)$; see Appendix B.

[8] Note that if s is not a QNM, then the solution (40) cannot be expressed in terms of the desired spectral decomposition formula; see discussion in Sec. VI B.

$$\psi_- = \sum_{m=1}^{\infty} \frac{I_{-m}}{(1-\sigma)^m}, \qquad \psi_+ = \sum_{k=0}^{\infty} I_k (1-\sigma)^k, \tag{44}$$

we find that ψ_- corresponds to a function which is analytic outside $\bar{\mathbf{C}}$ [the closure of the circle $\mathbf{C}$, cf. (32)], while ψ_+ is analytic inside $\mathbf{C}$. Hence, there is no annulus in the complex σ plane about the point $\sigma = 1$ within which the formal Laurent series $\psi = \psi_- + \psi_+$ would converge. Nevertheless, ψ_- and ψ_+ can be extended analytically into exterior and interior of $\mathbf{C}$, respectively, and there $(\psi_- + \psi_+)$ describes the complex continuation of a function ψ that satisfies (41). Note that the complex extension of ψ_- is a function with singularities at $\sigma \in \{0, 1\}$ and a branch cut discontinuity along the real interval $\sigma \in (0, 1)$. Likewise, ψ_+ is a function with singularities at $\sigma \in \{0, \infty\}$ and a branch cut discontinuity along the real interval $\sigma \in (-\infty, 0)$. Thus, the resulting function ψ possesses a branch cut discontinuity along the real interval $\sigma \in (-\infty, 1)$.

As a solution to (41), the function $\psi = \psi_- + \psi_+$ can be written in terms of ϕ as

$$\psi(\sigma; s) = \phi(\sigma; s)[C(s)\Pi(\sigma; s) + c(s)] \tag{45}$$

with s-dependent constants of integration $C(s)$ and $c(s)$ and where

$$\begin{aligned}\Pi(\sigma; s) &= \int_{1/2}^{\sigma} e^{s/\tilde{\sigma}} \frac{[\tilde{\sigma}(1-\tilde{\sigma})]^{\lambda-s-1} d\tilde{\sigma}}{\tilde{\sigma}^{3\lambda+1}[\phi(\tilde{\sigma}; s)]^2} \\ &= \int_{1/2}^{\sigma} e^{-s/\tilde{\sigma}} \frac{[\tilde{\sigma}(1-\tilde{\sigma})]^{\lambda-s-1} d\tilde{\sigma}}{\tilde{\sigma}^{1-2s-\lambda}[\Phi(\tilde{\sigma}; s)]^2}.\end{aligned} \tag{46}$$

With the convenient lower integration bound $1/2$, the function Π can be analytically extended for $0 < \sigma < 1$ from the right half-plane $\Re(s) > 0$ onto the left half-plane $\Re(s) < 0$. We remark that based on the aforementioned considerations it appears difficult to assess with certainty that the function ψ, when considered at *real* $\sigma \gtrsim 0$, is C^∞-regular at $\sigma = 0$ for $\Re(s) > 0$. This property would be essential to qualify ψ as one of the two linearly independent homogeneous solutions to (41) that, according to the definition in [13], constitute a Wronskian determinant whose zeros determine the set of QNMs. To show that ψ is C^∞-regular at $\sigma = 0$ would mean that we have to perform a complex continuation of ψ_- from the annulus $\{\sigma \in \mathbb{C} : |1-\sigma| > 1\}$ to *real* $\sigma \gtrsim 0$. As values of ψ_- anywhere inside the annulus are only given numerically, it appears extremely difficult to provide a decent analytical expansion of ψ_- as required. In Sec. IV D 1, we return to this issue but remark here that instead of the function ψ being considered, we concentrate in the following on the corresponding sequence $\{I_k\}$ which is defined through the specific asymptotics given in (42).

We now develop a higher-order approximation of the asymptotic expansion $(k \to +\infty)$ of the coefficients I_k, as they will be an essential ingredient in the solution of the Laplace transformed equation to be derived in Sec. IV A. For $k \gg 1$, we write

$$I_k = e^{-\kappa\sqrt{k}} k^\zeta A_k \tag{47}$$

where the coefficients A_k are given in terms of a regular function A defined on an ε neighborhood about the origin,

$$A_k = A\left(\frac{1}{\sqrt{k}}\right), \qquad A(x) = 1 + \sum_{j=1}^{\infty} \mu_j x^j. \tag{48}$$

Now, the expression (47) may be inserted into a slightly rearranged version of the recurrence relation (42), thus obtaining:

$$\begin{aligned}&\alpha_k \left(1 + \frac{1}{k}\right)^\zeta e^{-\kappa(\sqrt{k+1}-\sqrt{k})} A_{k+1} + \beta_k A_k \\ &\quad + \gamma_k \left(1 - \frac{1}{k}\right)^\zeta e^{-\kappa(\sqrt{k-1}-\sqrt{k})} A_{k-1} = 0.\end{aligned} \tag{49}$$

If we now consider (48) and expand (49) in terms of $1/\sqrt{k}$ about $k = \infty$, we can successively determine the μ_j's through the method of equating the coefficients. The first two terms amount to

$$\begin{aligned}\mu_1 &= \frac{1}{48\sqrt{s}}[8s(3+2s) - 9 - 48\ell(\ell+1)], \\ \mu_2 &= \frac{1}{4608s}[-135(1+16s) + 32(9\ell(\ell+1)(-1+8\ell(\ell+1)) \\ &\quad -72(\ell+\ell^2-\lambda)s - 3(21+16\ell(\ell+1)-48\lambda)s^2 \\ &\quad +60s^3+8s^4)].\end{aligned} \tag{50}$$

In this manner, all coefficients μ_j (and hence the function A) are completely fixed. A sample of the function A for $\lambda = \ell = 0$ and $s = 1 + i$ is displayed in the left panel of Fig. 4.

In our numerical computations, we determine, for given values of λ, ℓ and s, the coefficients $\{\mu_j\}_{j=1}^{2J_{\max}}$ for some integer $J_{\max}$ with high numerical precision. Thanks to the `Series` command in MATHEMATICA, values of $J_{\max}$ around 40 can easily be chosen. After the computation of the μ_j's, the function A is approximated by a diagonal Padé approximant

$$A_{\text{Pade}}(x) = \frac{\sum_{j=0}^{J_{\max}} p_j x^j}{1 + \sum_{j=1}^{J_{\max}} q_j x^j} \tag{51}$$

where the coefficients p_j, q_j are determined such that

$$\frac{d^j A_{\text{Pade}}}{dx^j}(0) = \frac{d^j A}{dx^j}(0) = j!\mu_j \quad \text{for } j = 0, \ldots, 2J_{\max}, \tag{52}$$

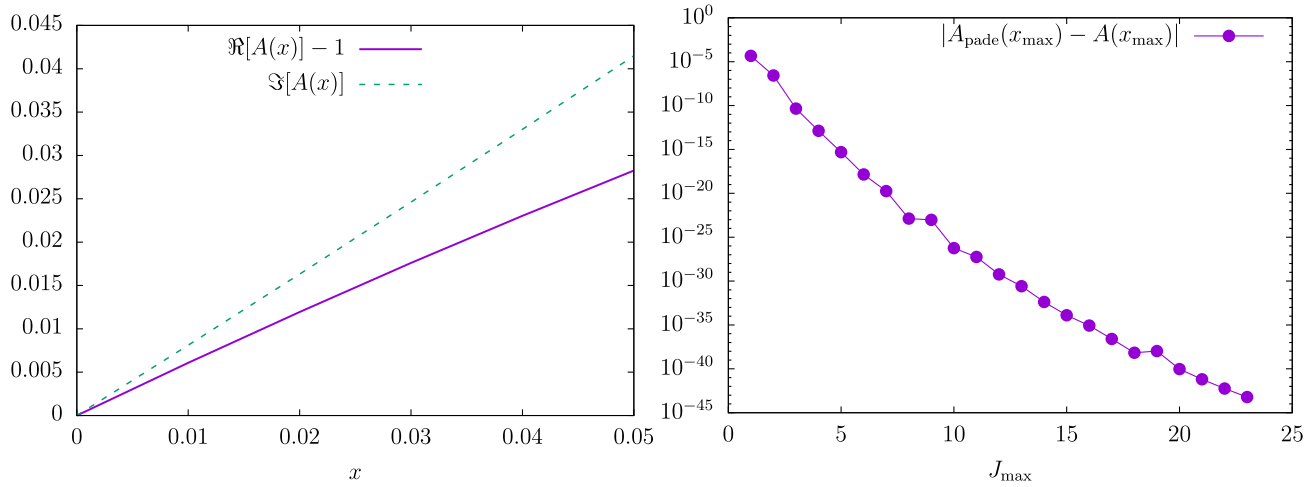

FIG. 4. Left panel: within the interval $x\in[0,x_{\rm max}]$ with $x_{\rm max}=0.05$, the function $A=A(x)$ [cf. (47), (48), (51)] is shown for $\ell=\lambda=0$ and the Laplace parameter $s=1+i$. The values $x\le 0.05$ correspond to the indexes $k\ge k_{\rm max}=x_{\rm max}^{-2}=400$. Right panel: maximal deviation, obtained for $x=x_{\rm max}$, of the approximation function $A_{\rm Pade}$ [cf. (51), (52)] from the function A, in dependence of the expansion order $J_{\rm max}$.

with $\mu_0=1$, cf. (48). In this way, we create a highly accurate approximation $A_{\rm Pade}$ of the function A, from which we may obtain approximative values of the two coefficients $I_{k_{\rm max}+1}$ and $I_{k_{\rm max}}$ for some large index $k_{\rm max}$ from the relation (47). The high order and the corresponding extreme accuracy of the Padé approximation allows us to get away with rather moderate values of e.g. $k_{\rm max}\sim 400$; see the right panel of Fig. 4.

We proceed with the determination the coefficients I_k for $k\in\{-1,\ldots,k_{\rm max}-1\}$ from the backwards recurrence relation

$$I_{k-1}=-\frac{1}{\gamma_k}(\alpha_k I_{k+1}+\beta_k I_k),\quad k=k_{\rm max},\ldots,0. \tag{53}$$

Note that for $s\notin\mathbb{Z}$, the coefficients γ_k do not vanish, cf. (30). The I_k's for $k\le -2$ are not needed in the sequel, although they also follow from (53).

A note at the end of this section seems appropriate. The aforementioned asymptotics (36), (47) and (48) arise as the result of a particular ansatz which appears to work by means of the asymptotic expansion of (29) and (42) and the subsequent application of the method of equating the coefficients. That is to say that we do not intend to provide a full proof of the aforementioned statements, but rather describe a particular route towards the solution of the ODE (12) in terms of a Taylor expansion analysis.

B. Unique solutions of the Laplace transformed wave equation

For the construction of solutions to (12) for prescribed values ℓ, λ and $s\in\mathbb{C}$, we first consider two notations which will be useful in the sequel. For a sequence $\{a_k\}_{-\infty}^{\infty}$ we define the discrete derivative via the difference

$$a'_k:=a_{k+1}-a_k. \tag{54}$$

Moreover, for two sequences $\{a_k\}_{-\infty}^{\infty}$ and $\{b_k\}_{-\infty}^{\infty}$, we introduce the discrete Wronskian determinant by

$$W_k(\{a_k\},\{b_k\}):=a'_k b_k-a_k b'_k=a_{k+1}b_k-a_k b_{k+1}. \tag{55}$$

In the following, we discuss $W_k(\{H_k\},\{I_k\})$ with the sequences $\{H_k\}_{-\infty}^{\infty}$ and $\{I_k\}_{-\infty}^{\infty}$ considered in the previous section, which we abbreviate by simply writing W_k. From (29) and (42), we find

$$\begin{aligned}0&=I_k(\alpha_k H_{k+1}+\beta_k H_k+\gamma_k H_{k-1})\\&\quad-H_k(\alpha_k I_{k+1}+\beta_k I_k+\gamma_k I_{k-1})\\&=\alpha_k W_k-\gamma_k W_{k-1},\end{aligned}$$

i.e.

$$W_k=\frac{\gamma_k}{\alpha_k}W_{k-1}. \tag{56}$$

We concentrate again on $s\notin\mathbb{Z}_0^-$ (see footnote 6). Also, we assume here that s is not a QNM; these are just the values at which the construction to be described will fail; see Secs. IV D and IV E. Then we obtain nonvanishing regular values W_k for $k\ge -1$:

$$W_{-1}=I_{-1},\qquad W_k=I_{-1}\prod_{j=0}^{k}\frac{\gamma_j}{\alpha_j}\quad\text{for } k\ge 0 \tag{57}$$

since $\alpha_j\neq 0$ and $\gamma_j\neq 0$ for $j\ge 0$. Moreover, we have $H_k=0$ for $k<0$ and hence $W_k=0$ for $k<-1$. With the scaling condition $H_0=1$, cf. (31), we get $W_{-1}=I_{-1}$. Note that in the following, the term

$$\frac{1}{\alpha_j}\prod_{m=0}^{j}\frac{\alpha_m}{\gamma_m}=\frac{j!\Gamma(s)\Gamma(s+\lambda)\Gamma(j+s-\lambda+1)}{\Gamma(j+s+1)\Gamma(s-\lambda+1)\Gamma(j+s+\lambda+1)}$$
$$=j^{-(2\lambda+s)}\frac{\Gamma(s)\Gamma(s+\lambda)}{\Gamma(s-\lambda+1)}[1+O(j^{-1})] \tag{58}$$

occurs frequently. Now we can address the solution to the inhomogeneous Laplace transformed wave equation (12). Let us start with the assumption that the initial data be of polynomial form, that is, for some integer $K_{\max}$ we may write

$$V(0,\sigma)=V_0(\sigma)=\sum_{k=0}^{K_{\max}-1}v_k(1-\sigma)^k$$
$$V_{,\tau}(0,\sigma)=\dot{V}_0(\sigma)=\sum_{k=0}^{K_{\max}-1}w_k(1-\sigma)^k. \tag{59}$$

Later in the text, we will relieve this restriction to allow for initial data that are analytic for $\sigma\in[0,1]$.

Writing accordingly the Laplace transform $\hat{V}$ as

$$\hat{V}(\sigma;s)=\sum_{k=0}^{\infty}a_k(1-\sigma)^k, \tag{60}$$

we arrive via Eq. (12) at the recursion relation

$$\alpha_k a_{k+1}+\beta_k a_k+\gamma_k a_{k-1}=B_k,\quad a_k=0\ \text{ for } k<0, \tag{61}$$

with

$$B_k=(k+1)v_{k+1}-2(2k+s+1)v_k$$
$$+(2k+\lambda+s)v_{k-1}-2w_k+w_{k-1} \tag{62}$$

and $B_k=0$ for $k<0$ and $k>K_{\max}$. It turns out that

$$a_k=c_kH_k+C_kI_k \tag{63}$$

with the condition

$$c_k'H_k+C_k'I_k=0, \tag{64}$$

where the coefficients c_k and C_k are to be determined, is a well-functioning ansatz for all $k\in\mathbb{Z}$ for which $W_k\neq 0$, i.e. for $k\geq -1$. Note that from (63) we learn that $C_k=0$ for $k<0$ since then $a_k=H_k=0$ and $I_k\neq 0$. Moreover, the coefficients c_k are arbitrary and undetermined for $k<0$. In addition, when looking at (64) for $k=-1$ and taking $H_{-1}=C_{-1}=0\neq I_{-1}$ into account, we see that also $C_0=0$.

If we now insert (63) into (61), thereby considering (29), (42) and (64), we get for $k\geq -1$:

$$\alpha_k(H_{k+1}c_k'+I_{k+1}C_k')=B_k. \tag{65}$$

As $\alpha_{-1}=B_{-1}=0$, this equation is trivially satisfied for $k=-1$. For $k\geq 0$, Eqs. (64) and (65) can be written as

$$\begin{pmatrix}H_k & I_k\\ H_{k+1} & I_{k+1}\end{pmatrix}\begin{pmatrix}c_k'\\ C_k'\end{pmatrix}=\begin{pmatrix}0\\ \frac{B_k}{\alpha_k}\end{pmatrix} \tag{66}$$

with the solution

$$c_k'=\frac{I_kB_k}{\alpha_kW_k},\qquad C_k'=-\frac{H_kB_k}{\alpha_kW_k}, \tag{67}$$

i.e. by virtue of $C_0=0$,

$$c_k=c_0+\sum_{j=0}^{k-1}\frac{I_jB_j}{\alpha_jW_j},\qquad C_k=-\sum_{j=0}^{k-1}\frac{H_jB_j}{\alpha_jW_j}. \tag{68}$$

In order to determine the constant c_0 appearing in this context, we require that $a_k\sim I_k$ as $k\to\infty$ for polynomial initial data. This ensures that for $\Re(s)>0$ the Laplace transform $\hat{V}$ is C^∞ at $\sigma=0$ and does not blow up exponentially there. We remark that only such solutions $\hat{V}$ can be taken to build up the wave field V via the Bromwich integral (15).

From (68) we learn that for polynomial initial data (60) we have for $k>K_{\max}$:

$$c_k=c_0+\sum_{j=0}^{K_{\max}}\frac{I_jB_j}{\alpha_jW_j}=:c^*=\text{const}, \tag{69}$$

$$C_k=-\sum_{j=0}^{K_{\max}}\frac{H_jB_j}{\alpha_jW_j}=\text{const} \tag{70}$$

Now, the requirement $a_k\sim I_k$ as $k\to\infty$ means that c^* must vanish [cf. (63)], which leads us with (57) to the final solution

$$a_k=-\frac{1}{I_{-1}}\left(H_k\sum_{j=k}^{K_{\max}}\frac{I_jB_j}{\alpha_j}\prod_{m=0}^{j}\frac{\alpha_m}{\gamma_m}+I_k\sum_{j=0}^{k-1}\frac{H_jB_j}{\alpha_j}\prod_{m=0}^{j}\frac{\alpha_m}{\gamma_m}\right). \tag{71}$$

In this expression, the limit $K_{\max}\to\infty$ is easily performed, allowing for initial data whose complex extension is analytic within the circle $\mathbf{C}$. Indeed, if we write

$$a_k=\sum_{j=0}^{\infty}G_{kj}B_j \tag{72}$$

with

$$G_{kj} = -\frac{1}{I_{-1}} \times \begin{cases} \dfrac{I_k H_j}{\alpha_j} \displaystyle\prod_{m=0}^{j} \frac{\alpha_m}{\gamma_m} & \text{for } j < k \\ \dfrac{H_k I_j}{\alpha_j} \displaystyle\prod_{m=0}^{j} \frac{\alpha_m}{\gamma_m} & \text{for } j \geq k \end{cases}, \tag{73}$$

we obtain the implication

$$\lim_{j\to\infty} \left| \frac{B_{j+1}}{B_j} \right| = \epsilon \Rightarrow \lim_{j\to\infty} \left| \frac{G_{k(j+1)} B_{j+1}}{G_{kj} B_j} \right| = \epsilon, \tag{74}$$

and hence convergence in (72) for all $k \geq 0$ in the case of initial data which are analytic within the circle $\mathbf{C}$ and thus satisfy $\epsilon < 1$. Note that (72) presents a representation of the solution a_k of (61) in terms of the discrete Green's function G_{kj} given in (73). This name is justified because of the relation

$$\alpha_k G_{(k+1)m} + \beta_k G_{km} + \gamma_k G_{(k-1)m} = \delta_{km}, \tag{75}$$

which follows from (72) and (61) for $B_j = \delta_{jm}$.

Let us now discuss the case in which the initial data are analytic for all $\sigma \in [0,1]$ but whose complex extension is not analytic within the circle $\mathbf{C}$, i.e. $\epsilon > 1$ in (74). Then the series (72) does not converge. Yet, in order to determine a definite limit even in this case we introduce

$$a_k(x) = \sum_{j=0}^{\infty} G_{kj} B_j x^j \tag{76}$$

which is a Taylor series that converges for $|x| < 1/\epsilon$. The corresponding function $a_k(x)$ may, however, be defined on the entire interval $x \in [0,1]$, and we obtain a good approximation again via a diagonal Padé approximant

$$a_k^{\text{Pade}}(x) = \frac{\sum_{j=0}^{j_{\max}} p_j x^j}{1 + \sum_{j=1}^{j_{\max}} q_j x^j} \tag{77}$$

where the coefficients p_j, q_j [different from the ones in (51)] are determined such that

$$\frac{d^j a_k^{\text{Pade}}}{dx^j}(0) = \frac{d^j a_k}{dx^j}(0) = j! G_{kj} B_j \tag{78}$$

for $j = 0, \ldots, 2j_{\max}$. The values $a_k^{\text{Pade}}(x=1)$ serve us as good approximations for the a_k, and we thus obtain the Taylor series (60) which describes a unique solution $\hat{V}$ to the inhomogeneous ODE (12). As the coefficients B_j of the initial data appearing in (12) are characterized by a specific radius $1/\epsilon < 1$ of convergence of the associated Taylor series, we expect that also the coefficients a_k are subject to that convergence radius, meaning that (60) is valid only for $|1-\sigma| < 1/\epsilon$. Similar to the treatment above, we establish $\hat{V}(\sigma; s)$ in the entire range $\sigma \in [0,1]$ by utilizing once more a diagonal Padé-approximant (here with respect to the coordinate σ):

$$\hat{V}_{\text{Pade}}(\sigma; s) = \frac{\sum_{j=0}^{k_{\max}/2} p_j (1-\sigma)^j}{1 + \sum_{j=1}^{k_{\max}/2} q_j (1-\sigma)^j}, \tag{79}$$

where the coefficients p_j, q_j [different from the ones in (51) and (77)] are determined such that $\hat{V}_{\text{Pade}}$ agrees with $\hat{V}$ to the order $k_{\max}$, which amounts to the conditions

$$\frac{d^k \hat{V}_{\text{Pade}}}{d\sigma^k}(1; s) = \frac{d^k \hat{V}}{d\sigma^k}(1; s) = (-1)^k k! a_k \quad \text{for } k = 0, \ldots, k_{\max}. \tag{80}$$

The corresponding solutions $\hat{V}(\sigma; s)$ are analytic for $\sigma \in (0,1]$ and still C^∞ at $\sigma = 0$. Computed at the line (16), they are perfectly suited to express the wave-field $V(\tau, \sigma)$ via the Bromwich integral (15), as is done in Secs. IV C and A.

C. Numerical evaluation of the Bromwich integral

Before proceeding further on the way towards the desired spectral decomposition of the wave field, we investigate as a first application and test of the procedure described in Sec. IV B the numerical evaluation of the inverse Laplace transform. To this end, we compute the function $\hat{V}(s)$ for values of s located on the path Γ_1 [see Fig. 2 and Eq. (16)] and construct from these the solution to the wave Eq. (9) in the form of the Bromwich integral (15). While Appendix A contains more details regarding these calculations, we concentrate here on the discussion of the numerical behavior of this solution technique.

Figure 5 brings two examples of the time evolution for initial data prescribed by $V_0(\sigma) = 1$ and $\dot{V}_0(\sigma) = 0$. The first one represents a scalar perturbation with parameters $\lambda = 0$ and $\ell = 0$ while the second one corresponds to an electromagnetic perturbation with $\lambda = -1$ and $\ell = 2$. The Bromwich integral is evaluated along the line $\Re(s) = 1/10$, and we plot $V(\sigma = 0, \tau)$, i.e. the dynamics of the wave field at $\mathcal{I}^+$. The time evolution of the first example shows an early tail decay whereas the second one possesses a long-lasting ring-down phase.

In the figures, it becomes apparent that the Bromwich integral method, when computed along the path Γ_1, does not seem to be well suited for the study of the wave's late time behavior. This observation is a consequence of the systematic errors introduced by the discretization of the integral. As discussed in the Appendix A, within our approach the numerical solution tends to zero exponentially which prohibits the resolution of the tail at very large times. In contrast, the spectral decomposition of the wave field, to be derived in the sequel, does provide in principle an arbitrarily accurate description of the very late time tail. Note that all the results in this section were obtained with

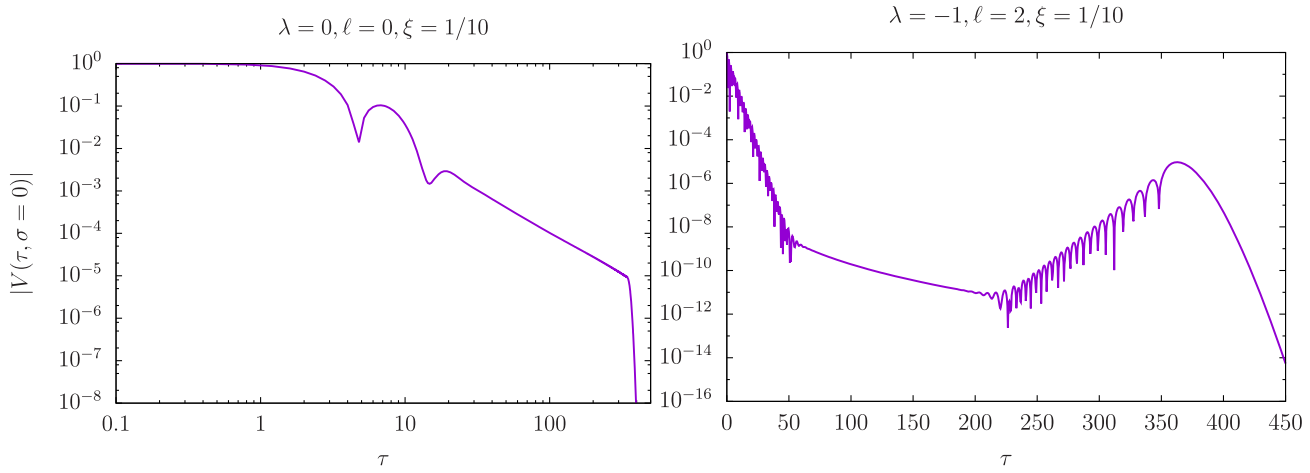

FIG. 5. Solution of the Barden-Press equation (9) via the Bromwich integral method (15) for the initial data $V_0(\sigma) = 1$, $\dot{V}_0(\sigma) = 0$. Left panel: time evolution of a scalar perturbation with parameters $\lambda = 0$ and $\ell = 0$. Right panel: electromagnetic perturbation with parameters $\lambda = -1$ and $\ell = 2$. Both fields are evaluated at $\mathcal{I}^+$, i.e. at $\sigma = 0$, and the Bromwich integral is performed along the line $\Re(s) = 1/10$ (see Fig. 2).

the fixed Taylor resolution $k_{\max} = 500$, $J_{\max} = 10$. Moreover, the resolution for the numerical evaluation of the integral (15) was set to $n_\chi = 200$ (see Appendix A).

D. Quasinormal modes

1. Approach within the Cauchy formulation

We start by reviewing the definition of QNMs as usually expressed in the literature (see, for instance, [13]) and describe why a direct computation according to this characterization seems to pose essential technical difficulties when analysed in the context of perturbations in asymptotically flat black-hole spacetimes.

Working with the Cauchy coordinates $\{\bar{t}, x\}$ introduced in Sec. III C, one first considers in the region $\Re(\bar{s}) > 0$ the homogeneous equation (24) which has two linearly independent solutions $F^{\pm}(x; \bar{s})$, chosen in such a way that they stay bounded as $x \to \pm\infty$. More specifically, the solutions satisfy

$$\lim_{x\to\pm\infty} |e^{\pm x\bar{s}} F^{\pm}(x; \bar{s})| = 1. \tag{81}$$

Then one constructs the Wronskian determinant[9]

$$\bar{\mathcal{W}}(\bar{s}) = F^+_{,x}(x; \bar{s}) F^-(x; \bar{s}) - F^-_{,x}(x; \bar{s}) F^+(x; \bar{s}) \tag{82}$$

and analytically extends it onto the half-plane $\Re(s) < 0$. The QNMs are then defined as the values $\bar{s}_n$ for which $\bar{\mathcal{W}}(\bar{s}_n) = 0$.

[9]For equations of the form (24), the Wronskian determinant does not depend on the coordinate x [14].

In order to compute $\bar{\mathcal{W}}$ explicitly as defined above,[10] we relate the two functions $F^{\pm}$ to solutions $\Omega(s)$ of the homogeneous Laplace transformed equation $\mathbf{A}(s)\Omega(s) = 0$ [cf. (27) and (41)] appearing in our hyperboloidal framework. From the exponential fall-off of F^- when $x \to -\infty$ we conclude that F^- can be written in terms of ϕ. Concretely, with the help of Eq. (23) and the regularity condition (81) we find

$$F^-(x(\sigma); \bar{s}) = \frac{e^{2\bar{s}}}{2} \Xi(\sigma; \bar{s}) \phi(\sigma; 2\bar{s}) \tag{83}$$

with the function Ξ defined in (26). For the second solution F^+ that needs to satisfy the regularity condition (81), we have to take

$$F^+(x(\sigma); \bar{s}) = \Xi(\sigma; \bar{s}) \Psi(\sigma; 2\bar{s}), \tag{84}$$

where

$$\Psi(\sigma; s) = \frac{s}{2} \Phi(0; s) \phi(\sigma; s) \int_0^\sigma e^{s/\tilde{\sigma}} \frac{[\tilde{\sigma}(1-\tilde{\sigma})]^{-(s+1)} d\tilde{\sigma}}{\tilde{\sigma}[\phi(\tilde{\sigma}; s)]^2} \tag{85}$$

is a solution to (41) that is C^∞-regular at $\sigma = 0$ for all $\Re(s) > 0$ (recall that $\lambda = 0$ here). Note that once more the function Φ appears which was defined in (38).

We now can write the Wronskian determinant $\bar{\mathcal{W}}(s)$ in (82) as

[10]As mentioned in Sec. III C, the comparison between both approaches is performed for $\lambda = 0$. We furthermore recall that the Laplace parameters are related by $s = 2\bar{s}$.

$$\bar{\mathcal{W}}(\bar{s}) = \frac{e^{2\bar{s}}}{2}\sigma^2(1-\sigma)\Xi(\sigma;\bar{s})^2\mathcal{W}(\sigma;2\bar{s}) \tag{86}$$

with $\mathcal{W}(\sigma;s)$ being the Wronskian determinant formed from ϕ and Ψ:

$$\begin{aligned}\mathcal{W}(\sigma;s) &= \phi_{,\sigma}(\sigma;s)\Psi(\sigma;s) - \Psi_{,\sigma}(\sigma;s)\phi(\sigma;s)\\ &= \frac{s}{2}\Phi(0;s)e^{s/\sigma}\sigma^{-(s+2)}(1-\sigma)^{-(s+1)}.\end{aligned} \tag{87}$$

We finally find

$$\bar{\mathcal{W}}(\bar{s}) = 2\bar{s}e^{2\bar{s}}\Phi(0;2\bar{s}), \tag{88}$$

which depends solely on $\bar{s}$, as expected. Following the discussion made after the introduction of $\Phi(\sigma;s)$ in (38), we see that $\bar{\mathcal{W}}(\bar{s})$ is well defined for $\Re(\bar{s}) > 0$. However, the values $\Phi(\sigma = 0; 2\bar{s})$ are involved which appear to be determinable only numerically to some accuracy. Now, they are supposed to constitute a function that is well-defined on the right complex half-plane $\Re(\bar{s}) > 0$. In order to determine the set of QNMs it would then be necessary to continue this function analytically to the left half-plane $\Re(\bar{s}) < 0$ and identify there its set of zeros. As an example, if we simply had $\Phi(\sigma; 2\bar{s}) = e^{-\bar{s}/\sigma} + 1 + \bar{s}$ then we would get $\Phi(\sigma = 0; 2\bar{s}) = 1 + \bar{s}$ for $\Re(\bar{s}) > 0$, and this can of course trivially be analytically expanded to the entire $\bar{s}$ plane, despite the fact that $\Phi(0; 2\bar{s})$ does not exist for $\Re(\bar{s}) < 0$. On the technical side it appears extremely complicated to provide a reasonable and sound, sufficiently accurate continuation of the numerically determined function values $\Phi(\sigma = 0; 2\bar{s})$ onto the left half-plane. Hence we feel that the concrete determination according to the usual definition of QNMs given in [13] needs to be performed in some different, indirect manner.

In the next section, we provide a working definition of the QNMs which results in the same expressions as the ones used by Leaver in his approach utilizing continued fractions [16]. In particular, we derive that the QNMs can be characterized through the vanishing of the Wronskian determinant

$$\mathbb{W}(\sigma;s) = \phi_{,\sigma}(\sigma;s)\psi(\sigma;s) - \psi_{,\sigma}(\sigma;s)\phi(\sigma;s) \tag{89}$$

of the two solutions ϕ and ψ to (41) that were discussed extensively in Sec. IV A. Note that in order to analyse whether this approach is equivalent to definition of QNMs given in [13] it would be necessary to show that Ψ is proportional to ψ, i.e. to prove that ψ, when considered for real $\sigma \gtrsim 0$, is C^∞-regular at $\sigma = 0$ for $\Re(s) > 0$. Even a mere numerical check of this equivalence would pose again substantial technical difficulties; see discussion in Sec. IV A.

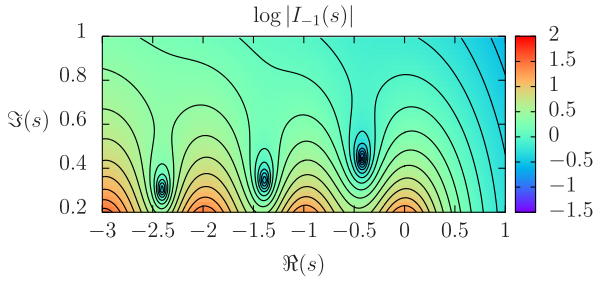

FIG. 6. Contour plot of the function $\log|I_{-1}(s)|$ in the complex s plane for $\lambda = \ell = 0$. The centres of the concentrically arranged closed curves are the locations of the quasinormal modes s_n, shown here for $n \in \{0, 1, 2\}$. At these points, $I_{-1}(s)$ vanishes.

2. Quasinormal modes as zeros of the discrete Wronskian determinant

Quasinormal modes s_n are specific values in the complex s plane for which the procedure, described in Sec. IV B to determine a unique solutions of the Laplace transformed wave equation, fails. The reason for the failure is given by the fact that

$$I_{-1}(s_n) = 0, \tag{90}$$

from which it follows that the construction (72), (73) cannot be performed. The zeros of the function $I_{-1}(s)$ have always been found to be distributed discretely in the left half-plane $\Re(s) < 0$. Figure 6 shows a contour plot of $I_{-1}(s)$ for $\lambda = \ell = 0$.

We immediately arrive at several equivalent characterizations:

(i) For $s = s_n$ as a QNM, the discrete Wronskian determinant $W_k(\{H_k\}, \{I_k\})$ vanishes for all $k \in \mathbb{Z}$. This follows directly from (57).

(ii) For $s = s_n$ as a QNM, the Wronskian determinant $\mathbb{W}(\sigma; s_n)$, as defined in (89) in terms of the two solutions ϕ and ψ introduced in Sec. IV A, vanishes for all $\sigma \in [0, 1]$.

With (90) we obtain that $I_k = 0$ for all $k < 0$ [see (53) *with* $\alpha_{-1} = 0$, cf. (30)] and hence $I_k = I_0 H_k$; i.e., the two sequences $\{H_k\}$, $\{I_k\}$ are linearly dependent. As a consequence, the associated functions ϕ and ψ satisfy $\psi = I_0\phi$ and, hence, $\mathbb{W}(\sigma; s_n) = 0$, cf. (89).

(iii) A QNM s_n is defined by the existence of a nontrivial solution $\phi = \phi_n$ to (27) that possesses a Taylor expansion (28) with rapidly decreasing coefficients. That is to say that there is, for each $\nu \in \mathbb{N}$, a positive constant C_ν such that for all $k \in \mathbb{N}$,

$$|H_k(s_n)| < \frac{C_\nu}{k^\nu}. \tag{91}$$

This formulation follows directly from the fact that $H_k = I_k/I_0 \sim e^{-\kappa\sqrt{k}}k^\zeta$ *for* $k \to \infty$; see (42).

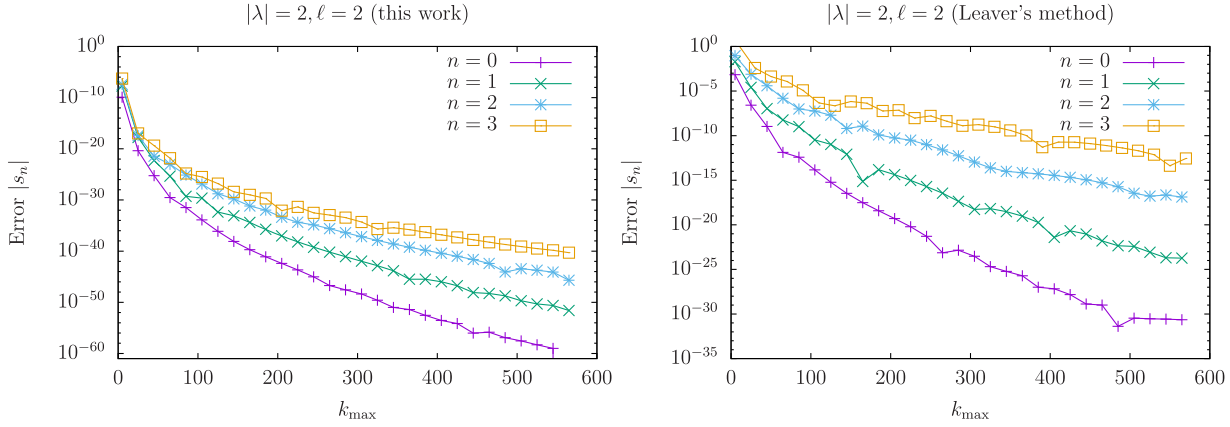

FIG. 7. Errors in the numerical determination of the quasinormal modes s_n, displayed as functions of the truncation number $k_{\max}$ for a gravitational perturbation with parameters $|\lambda| = 2$ and $\ell = 2$. The left panel shows the results according to the algorithm presented in this work (with $J_{\max} = 10$), while the right panel brings the corresponding value obtained with Leaver's method of continued fractions. It becomes apparent that the errors are drastically reduced by taking the asymptotic behavior (47), (48) of the coefficients I_k into account.

Among these three characterizations, point (iii) plays a preferred role. Points (i) and (ii) make use of the two sequences $\{H_k\}$ and $\{I_k\}$ of coefficients which cannot be defined in its entirety for $s \in \mathbb{Z}^-$; see discussion in Appendix C. This means that the negative integer, the so-called "algebraically special" QNMs $s_{(\ell)}$ [32] (to be treated in Appendix D), is excluded in points (i) and (ii) (in the definition of H_k and I_k in Sec. IV A we have set $s \notin \mathbb{Z}_0^-$). However, point (iii) still applies since the corresponding solutions $\phi_{(\ell)}$ are polynomials and satisfy therefore trivially this formulation. We conclude that (iii) should be regarded as generically valid definition of QNMs for perturbations in the asymptotically flat Schwarzschild spacetime.

For the numerical computation of the QNMs $s_n \notin \mathbb{Z}_0^-$, Leaver [16] has looked at the recursion relation

$$b_{k-1} = -\frac{\gamma_k}{\beta_k + \alpha_k b_k} \quad \text{with} \quad b_k := \frac{I_{k+1}}{I_k}, \tag{92}$$

through which the coefficients b_k can be written in terms of continued fraction expressions. Starting with $b_{k_{\max}} = 1$ for some very large value $k_{\max}$ and climbing down via (92), one obtains through the condition

$$0 = \frac{1}{I_0}(\alpha_0 I_1 + \beta_0 I_0 + \gamma_0 I_{-1}) = \alpha_0 b_0 + \beta_0$$

an equation that determines the QNMs s_n. In practice, this equation can be solved numerically using the `FindRoot`-command provided within Mathematica (see e.g. [36]). This method achieves in principle arbitrary precision. However, for very accurate calculations, extremely large vales $k_{\max}$ and a high internal working precision of the Mathematica notebook need to be chosen. The costs of this numerical calculation can be reduced drastically by making use of the approximation function A_{Pade} introduced in Sec. IV A above. As described therein, given a suitable expansion order $J_{\max}$ we can choose a moderate number $k_{\max}$ (say about 400) to obtain extremely accurate values I_k, in particular for I_{-1}. The zero s_n is then found by a Newton-Raphson scheme,

$$s_n = \lim_{j\to\infty} s_n^{(j)}, \qquad s_n^{(j+1)} = s_n^{(j)} - \frac{I_{-1}(s_n^{(j)})}{(\partial_s I_{-1})(s_n^{(j)})}, \tag{93}$$

where a suitable initial guess $s_n^{(0)}$ is needed. Note that for the numerical computations, the derivative $\partial_s I_{-1}$ can be approximated through a finite difference expression. An illustrative example demonstrating the accuracy and performance of this calculation in comparison with Leaver's method is shown in Fig. 7.

As an additional note, we remark that (41) has, for $s = s_n$ being a QNM, a second solution Λ which is linearly independent of ϕ_n. This solution Λ can be described similarly as ψ in Sec. IV A by a series $\{L_k\}_{-\infty}^{\infty}$ with

$$\alpha_k L_{k+1} + \beta_k L_k + \gamma_k L_{k-1} = 0,$$
$$\lim_{k\to\infty} L_k e^{-\kappa\sqrt{k}} k^{-\zeta} = 1, \tag{94}$$

as $\Lambda = \Lambda_+ + \Lambda_-$, where

$$\Lambda_- = \sum_{m=1}^{\infty} \frac{L_{-m}}{(1-\sigma)^m}, \qquad \Lambda_+ = \sum_{k=0}^{\infty} L_k (1-\sigma)^k. \tag{95}$$

Observe the diverging asymptotics of the L_k in (94), and hence Λ does not present a solution of the kind described in (iii) of the above characterization. Furthermore, as $L_k \neq 0$ for $k < 0$, Λ is singular at $\sigma = 1$. We conclude that the entirety of solutions to (27) is given by $\text{span}_{\mathbb{C}}(\phi_n)$. This point will be relevant below (see Sec. IV E).

We finally mention that, as a consequence of the symmetry relation (11), we find that the quasinormal modes s_n come in complex-conjugated pairs, s_n and s_n^*.

E. Quasinormal mode amplitudes

What happens to the solutions $\hat{V} = \hat{V}(s)$ of the inhomogeneous ODE (12), computed in Sec. IV B, if we approach a QNM, i.e. if $s \to s_n$ (here again $s_n \notin \mathbb{Z}^-$)? As then $I_{-1} \to 0$, Eq. (71) suggests that $\hat{V}(s)$ will diverge in this limit. Assuming that I_{-1} has merely a single zero at $s = s_n$,[11] the corresponding $\hat{V}(s)$ will possess a single pole at $s = s_n$. Accordingly, for values s close to s_n, we write

$$a_k(s) = \frac{h_k}{s - s_n} + g_k(s), \tag{96}$$

where h_k does not depend on s (in contrast to a_k and g_k). With the single polelike singularity of $\hat{V}$, the coefficient h_k is supposed to be the residue of a_k at s_n whereas $g_k(s)$ presents the secondary part of its Laurent series. That is to say that the coefficients $g_k(s)$ are supposed to be analytic in the vicinity of s_n. As will become clear below, the residues $\{h_k\}$ turn out to be proportional to $\{H_k(s_n)\}$, and the corresponding proportionality factor η_n will play a crucial role as the quasinormal mode amplitude in the desired spectral decomposition (3).

For the computation of η_n, let us start with initial data that are analytic within the circle $\mathbf{C}$ [i.e. for which $\epsilon < 1$ in (74)] and generalize the corresponding expression in a subsequent step. We formulate the recursion relation (61) as

$$\mathcal{A}(s) \cdot \{a_k\} = \{B_k\} \tag{97}$$

with the operator $\mathcal{A}(s)$ defined by

$$[\mathcal{A}(s) \cdot \{a_k\}]_k \coloneqq \alpha_k a_{k+1} + \beta_k a_k + \gamma_k a_{k-1}. \tag{98}$$

We now insert (96) into the relation (97), thereby rewriting (97) by using another operator $\mathcal{C}_n$ which is given through

$$\mathcal{A}(s) = \mathcal{A}(s_n) + (s - s_n)\mathcal{C}_n(s), \tag{99}$$

i.e.:

$$[\mathcal{C}_n(s) \cdot \{a_k\}]_k = (k+1)a_{k+1} - 2(2k + 1 + s + s_n)a_k + (2k + s + s_n + \lambda)a_{k-1}. \tag{100}$$

We obtain

$$[\mathcal{A}(s_n) + (s - s_n)\mathcal{C}_n(s)] \cdot \frac{\{h_k\}}{s - s_n} + \mathcal{A}(s) \cdot \{g_k\} = \{B_k\}, \tag{101}$$

which provides us in the limit $s \to s_n$ with the condition

$$\mathcal{A}(s_n) \cdot \{h_k\} \overset{!}{=} 0.$$

In the vicinity of the QNM s_n, i.e. for $0 < |s - s_n| < \varepsilon$ with some $\varepsilon \ll 1$, Eq. (96) describes the solution to (101) with vanishing and rapidly decreasing coefficients $\{h_k\}$, $\{g_k\}$ for $k < 0$ and $k \to \infty$ respectively. Hence, according to the fact that ϕ_n is the *only* C^∞-solution on the interval $\sigma \in [0, 1]$ (cf. discussion at the end of Sec. IV D), we have

$$h_k = \eta_n H_k(s_n) \tag{102}$$

with the QNM amplitude η_n as proportionality factor. We thus obtain

$$[\mathcal{A}(s_n) + (s - s_n)\mathcal{C}_n(s)] \cdot \frac{\{h_k\}}{s - s_n} = \eta_n \mathcal{C}_n(s) \cdot \{H_k(s_n)\}.$$

Equation (101) reads now

$$\mathcal{A}(s) \cdot \{g_k\}(s) = \{B_k\}(s) - \eta_n \mathcal{C}_n(s) \cdot \{H_k(s_n)\}. \tag{103}$$

For $s \neq s_n$, the solution of (103) can be found using the formula (71). In particular, we obtain

$$g_0(s) = -\frac{1}{I_{-1}} \sum_{j=0}^{\infty} \frac{I_j(B_j - \eta_n C_j)}{\alpha_j} \prod_{m=0}^{j} \frac{\alpha_m}{\gamma_m} \tag{104}$$

with

$$C_j \coloneqq [\mathcal{C}_n(s) \cdot \{H_k(s_n)\}]_j. \tag{105}$$

In the limit $s \to s_n$, we have $I_{-1} \to 0$, and (104) provides us with a finite value g_0 only if

$$\eta_n = \left[\frac{\sum_{j=0}^{\infty} \frac{H_j B_j}{\alpha_j} \prod_{m=0}^{j} \frac{\alpha_m}{\gamma_m}}{\sum_{j=0}^{\infty} \frac{H_j C_j}{\alpha_j} \prod_{m=0}^{j} \frac{\alpha_m}{\gamma_m}} \right]_{s=s_n}, \tag{106}$$

where we utilized that $I_j(s_n) = I_0(s_n)H_j(s_n)$. Note that the sum in the denominator is assured to converge since the addends are rapidly decreasing as $j \to \infty$ [see (42), (58), (100)]. The numerator can be written as $N = \sum_{j=0}^{\infty} G_j B_j$, and since $|G_{j+1}B_{j+1}/(G_j B_j)| \to \epsilon$ as $j \to \infty$ for our initial data that are analytic within the circle $\mathbf{C}$, we can again conclude convergence.

Now the case in which the initial data are analytic for all $\sigma \in [0, 1]$ but whose complex extension is not analytic within $\mathbf{C}$, i.e. $\epsilon > 1$ in (74), is treated as in Sec. IV B. We introduce $N(x) = \sum_{j=0}^{\infty} G_j B_j x^j$ and expand it to $x = 1$ with the help of an associated diagonal Padé approximant.

As an important quantity for the time range, within which the desired spectral decomposition formula (3) is

[11] This assumption has always been found to be realized.

valid, we now define the growth rate of the quasinormal mode amplitudes,

$$\nu_{\mathrm{QNM}}(\sigma) = \lim_{n\to\infty} \frac{\ln|\eta_n \phi_n(\sigma)|}{|\Re(s_n)|}. \tag{107}$$

The following statements hold:

(1) As

$$\nu_{\mathrm{QNM}}(\sigma) = \underbrace{\lim_{n\to\infty} \frac{\ln|\eta_n|}{|\Re(s_n)|}}_{=\nu_{\mathrm{QNM}}(1)} + \lim_{n\to\infty} \frac{\ln|\phi_n(\sigma)|}{|\Re(s_n)|},$$

the profile of $\nu_{\mathrm{QNM}}(\sigma)$ is universally given by the second term, while the first one is $\nu_{\mathrm{QNM}}(1)$ (which follows from the scaling condition $H_0 = 1$) and presents a constant shift depending on the initial data.

(2) For polynomial initial data (59), we obtain a universal growth rate $\nu_{\mathrm{QNM}}(\sigma)$. This follows from the fact that the numerator N in (106) is algebraic in s_n. Hence, we get

$$\begin{aligned}\nu_{\mathrm{QNM}}(1) &= -\lim_{n\to\infty} \frac{\ln\left|\sum_{j=0}^{\infty} \frac{H_j C_j}{\alpha_j} \prod_{m=0}^{j} \frac{\alpha_m}{\gamma_m}\right|_{s=s_n}}{|\Re(s_n)|} \\ &= -2,\end{aligned}$$

i.e. an expression that is independent of the particular choice of the polynomial initial data. Note that in our numerical investigations, this limit has been observed to be always -2, independently of the choices for λ and ℓ.

(3) Looking at (3), we see that the addends in the sum fall off exponentially for $\tau > \nu_{\mathrm{QNM}}(\sigma)$. Adding a similar argument with respect to the continuous integral part, we will be able to argue in Sec. VI, that this means full validity of the spectral decomposition formula (3) for such times.

F. The Laplace transform along the branch cut

Let us now consider the situation in which we approach the negative real axis within the complex s plane. Again we exclude, for the time being, integer s values, i.e. $s \in \mathbb{R}^-\backslash\mathbb{Z}^-$. (As mentioned in footnote 6, $s \in \mathbb{Z}^-$ will be treated in Appendix C.) Towards this axis, we can get from above or from below. In the first case, $\arg(s) \to \pi$, the corresponding $\kappa = 2\sqrt{s}$ with $\Re(\kappa) > 0$ tends to the positive imaginary axis, while in the latter one, $\arg(s) \to -\pi$, it runs towards the negative imaginary axis. Consequently, we obtain via the method presented in Sec. IV B for $s \in \mathbb{R}^-\backslash\mathbb{Z}^-$ the two solutions

$$\hat{V}^{\pm}(s) = \lim_{\varepsilon\to 0} \hat{V}(s \pm i|\varepsilon|)$$

with

$$\hat{V}^{\pm}(\sigma; s) = \sum_{k=0}^{\infty} a_k^{\pm} (1-\sigma)^k.$$

In the computation of the $a_k^{\pm}$ according to steps described in Sec. IV B, the coefficients B_k, H_k as well as $I_k^{\pm}$ are involved. Only the latter ones are different when getting to the negative real axis from above or from below; see asymptotics in (42).

Now, the symmetry condition (11) implies that

$$\hat{V}^-(s) = [V^+(s)]^*, \qquad a_k^- = [a_k^+]^*, \qquad I_k^- = [I_k^+]^*,$$

and the asymptotics (42) tells us that these quantities have, in general, both real and imaginary parts. With nonvanishing imaginary part of $\hat{V}^{\pm}(s)$ we conclude that the Laplace transform $\hat{V}(s)$ possesses, besides the simple poles at the QNMs s_n, a jump along the negative real axis, $s \in \mathbb{R}^-$:

$$\lim_{\varepsilon\to 0}[\hat{V}(s + i|\varepsilon|) - \hat{V}(s - i|\varepsilon|)] = \sum_{k=0}^{\infty} \underbrace{(a_k^+ - a_k^-)}_{=:d_k} (1-\sigma)^k.$$

Therefore, the negative real axis appears as a branch cut with respect to $\hat{V}(s)$. Now, as both a_k^+ and a_k^- satisfy the recursion relation (61), the coefficients $d_k = a_k^+ - a_k^-$ satisfy the homogeneous recurrence relation (29) and, moreover, $d_{-1} = 0$. Hence we have $d_k = d_0 H_k$ and thus:

$$\lim_{\varepsilon\to 0}[\hat{V}(s + i|\varepsilon|) - \hat{V}(s - i|\varepsilon|)] = -2\pi i \eta(s)\phi(s), \tag{108}$$

where we introduced $\eta(s) := -d_0/(2\pi i)$ which will appear in the spectral decomposition formula (3) as a branch cut amplitude. The computation of d_0 in terms of (71) yields

$$d_0 = a_0^+ - a_0^- = -\sum_{j=0}^{\infty} \frac{B_j}{\alpha_j} \prod_{m=0}^{j} \frac{\alpha_m}{\gamma_m} \underbrace{\left(\frac{I_j^+}{I_{-1}^+} - \frac{I_j^-}{I_{-1}^-}\right)}_{=:D_j},$$

where the coefficients D_j satisfy again the homogeneous recurrence relation (29) and, moreover, $D_{-1} = 0$. We conclude that $D_j = D_0 H_j$ and obtain, finally,

$$\eta(s) = \Im\left(\frac{I_0^+}{\pi I_{-1}^+}\right) \sum_{j=0}^{\infty} B_j \underbrace{\frac{H_j}{\alpha_j} \prod_{m=0}^{j} \frac{\alpha_m}{\gamma_m}}_{=:G_j}. \tag{109}$$

Again, this formula is valid as it stands for initial data that are analytic within the circle $\mathbf{C}$. For initial data that are analytic for all $\sigma \in [0,1]$ but whose complex extension is not analytic within $\mathbf{C}$, i.e. $\epsilon > 1$ in (74), we introduce once

more $N(x) = \sum_{j=0}^{\infty} G_j B_j x^j$ and expand it to $x = 1$ with the help of an associated diagonal Padé approximant.

For representative sample initial data, the magnitude $|\eta(s)\phi(\sigma; s)|$ is shown in Fig. 9.

Finally, let us define as in Sec. IV E the growth rate of the branch cut amplitudes,

$$\nu_{\mathrm{cut}}(\sigma) = -\lim_{n\to\infty}\left[\max_{-(n+1)\le s\le -n}\frac{\ln|\eta(s)\phi(\sigma;s)|}{|s|}\right]. \quad (110)$$

Note that the three statements at the end of Sec. IV E can be transferred to the growth rate of the branch cut amplitudes, with the second point modified by

$$-\lim_{n\to\infty}\left[\max_{-(n+1)\le s\le -n}\frac{1}{|s|}\ln\left|\Im\left(\frac{I_0^+}{\pi I_{-1}^+}\right)\right|\right] = -2.$$

It is interesting to note that in our numerical investigations of analytic initial data we observe that the growth rates ν_{QNM} and ν_{cut} of quasinormal mode amplitudes and branch cut amplitudes coincide. We believe that this is a consequence of the fact that these quantities arise from similar expressions, cf. (106) and (109). Henceforth we will simply use $\nu(\sigma)$ to denote the mutual growth rates ν_{QNM} and ν_{cut}.

G. Asymptotic expansion of the Laplace transform

In order to arrive at the spectral decomposition (3) in Sec. V via an appropriate deformation of the Bromwich integration path (see Fig. 2), we have to consider the contribution of the integral over the semicircular portion of Γ_2 in the complex s plane for $\tau > 0$. The two cases, positive and negative growth rates ν, have to be discussed separately.

Let us approach the matter with the auxiliary function

$$W(\tau) = \int_{-\infty}^{0} e^{s(\tau-\nu)}\sin(\omega s)ds = \Im\left[\frac{1}{\tau-\nu-i\omega}\right], \quad (111)$$

where we took in the desired formula (3) only the continuous integral part and, moreover, inserted for $\eta(s)\phi(\sigma; s)$ its asymptotics given through the growth rate ν, cf. (110). The phase ω (let us take $\omega > 0$) has been added in order to have a regular function W for $\tau > 0$. Note that the integral can only be performed for $\tau > \nu$, but the result is defined on the entire complex τ plane with single poles at $\nu \pm i\omega$.

Now, the integrand of the Bromwich integral (15) is given by $\hat{V}(\sigma; s)e^{s\tau}$. Consequently, we have to discuss here $\hat{W}(s)e^{s\tau}$ with

$$\hat{W}(s) = \mathcal{L}[W(\tau)](s) = \frac{1}{2i}(e^{-s(\nu+i\omega)}E_1[-s(\nu+i\omega)] - e^{-s(\nu-i\omega)}E_1[-s(\nu-i\omega)]),$$

where E_1 is an exponential integral. The function

$$f(z) = e^z E_1(z) \quad (112)$$

has a branch cut along the negative real axis in the complex z plane. Let us discuss this function as being defined on a Riemannian surface with infinitely many sheets. The crossing of the negative real axis means the analytic transition into a neighboring sheet. The function f is best described by another function

$$g\colon [0,\infty)\times(-\infty,\infty)\to\mathbb{C}, \qquad g(r,\varphi) = f(re^{i\varphi}), \quad (113)$$

where $z = re^{i\varphi}$ is assumed to be located in the kth sheet with $k = \lfloor(\varphi+\pi)/(2\pi)\rfloor$.[12] It turns out that

$$\lim_{r\to\infty}\frac{\ln|g(r,\varphi)|}{r} = \sin\left(\varphi+\frac{5\pi}{2}\right) \quad \text{for } \varphi\in\left(-\frac{5\pi}{2},-\frac{3\pi}{2}\right)$$
$$\lim_{r\to\infty}|g(r,\varphi)| = 0 \quad \text{for } \varphi\in\left(-\frac{3\pi}{2},\frac{3\pi}{2}\right)$$
$$\lim_{r\to\infty}\frac{\ln|g(r,\varphi)|}{r} = \sin\left(\varphi-\frac{3\pi}{2}\right) \quad \text{for } \varphi\in\left(\frac{3\pi}{2},\frac{5\pi}{2}\right). \quad (114)$$

Now, (112) means

$$\hat{W}(s) = \frac{1}{2i}[g(r,\varphi_+) - g(r,\varphi_-)] \quad (115)$$

with ($\omega > 0$),

$$r = |s|\sqrt{\nu^2+\omega^2}, \qquad \varphi_\pm = \arg(s) \pm [\arg(\nu+i\omega) - \pi].$$

Let us discuss $\nu < 0$ first. We have $-\pi < \arg(s) < \pi$ and $\pi/2 < \arg(\nu+i\omega) < \pi$. We conclude that

$$-\frac{3\pi}{2} < \varphi_+ < \pi, \qquad -\pi < \varphi_- < \frac{3\pi}{2},$$

and hence $|\hat{W}(s)|$ vanishes whenever $s\to\infty$ with $-\pi < \arg(s) < \pi$.

The case $\nu > 0$ is different. Now we have $\arg(\nu+i\omega)\in(0,\pi/2)$, and we get for $\arg(s) > \frac{\pi}{2} + \arg(\nu+i\omega)$:

$$|g(r,\varphi_-)| \sim e^{r\sin\epsilon_-}, \qquad \epsilon_- = \arg(s) - \arg(\nu+i\omega) - \frac{\pi}{2}.$$

Likewise, for $\arg(s) < -\arg(\nu+i\omega) - \frac{\pi}{2}$ we obtain

[12] Here we used the notation $\lfloor\cdot\rfloor$ for the floor function.

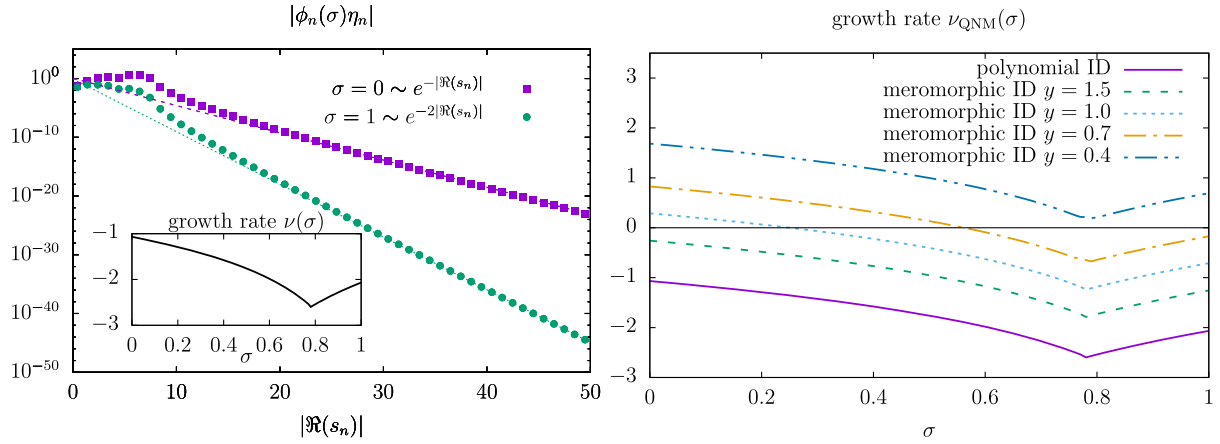

FIG. 8. Behavior of the residues $\eta_n\phi_n(\sigma)$ of the Laplace transform $\hat{V}(\sigma; s)$ at the quasinormal modes $\{s_n\}$ with prescribed parameters $\lambda = l = 0$. Left panel: for the polynomial initial data $V_0(\sigma) = \sigma^2(1-\sigma)^4$, $\dot{V}_0(\sigma) = 0$ the decay is shown for $\sigma = 0$ (at $\mathcal{I}^+$) and for $\sigma = 1$ (at the horizon). The inset brings the growth rate $\nu_{\rm QNM}(\sigma)$ for all $\sigma \in [0, 1]$. Right panel: comparison of the grow rate for the polynomial initial data against meromorphic initial data with single poles in the complex σ plane. Here, $V_0(\sigma) = 2\Re[(\sigma - \sigma_0)^{-1}]$, $\dot{V}_0(\sigma) = 0$, with $\sigma_0 = 0.5 + iy$. While polynomial initial data show a universal behavior, more generic initial data introduce a constant shift in the profile.

$$|g(r, \varphi_+)| \sim e^{r \sin \epsilon_+}, \qquad \epsilon_+ = -\arg(s) - \arg(\nu + i\omega) - \frac{\pi}{2}.$$

We conclude that, for $\nu > 0$, the function $\hat{W}(s)$ diverges exponentially as $|s| \to \infty$ when the limit is performed in the circular sector $|\arg(s)| > \frac{\pi}{2} + \arg(\nu + i\omega)$.[13] The strongest divergence is obtained for $|\arg(s)| \to \pi$; there we have $|\hat{W}| \sim e^{|s|\nu}$.

In Fig. 10, we display the behavior of the Laplace transform $\hat{V}(\sigma; s)$ in the half-plane $\Re(s) < 0$ for meromorphic initial data $V_0(\sigma) = 2\Re[(\sigma - \sigma_0)^{-1}]$, $\dot{V}_0(\sigma) = 0$ with single poles at σ_0 and σ_0^*. We take $\sigma_0 = 0.5 + iy$ and considered, in particular, the parameter $y = 0.7$. For these initial data, we obtain at $\sigma = 0.5$ a positive growth rate $\nu \approx 0.13$ (see Figs. 8 and 9). In Fig. 10, the existence of a circular sector $|\arg s| > 0.99\pi$ becomes apparent within which $\hat{V}(\sigma; s)$ diverges exponentially. As expected, the strongest divergence occurs for $|\arg s| = \pi$ with the rate ν.

We now turn to the deformation of the Bromwich integration path. Let us again consider the case $\nu < 0$ first. Although $|\hat{W}(s)| \to 0$ for $|s| \to \infty, |\arg(s)| < \pi$, we cannot simply apply Jordan's lemma in order to obtain vanishing contribution of the integral over the semicircular portion of Γ_2 in the complex s plane. The reason is that $\hat{W}$ possesses a branch cut along the negative s axis, a fact which is not included in the formulation of Jordan's lemma. Moreover, when considering $\hat{V}$ we see that it possesses poles at the QNMs $s = s_n$, accumulating at infinity. One might be reminded of the function $1/\sin(\pi s)$ with poles at real integer values. However, for $1/\sin(\pi s)$ the residues of the poles remain of finite magnitude as s tends to infinity. In contrast, the residues of $\hat{V}$ die out at the rate $e^{-\Re(s_n)\nu}$. Likewise, also the jump along the negative s axis falls off at the rate $e^{-s\nu}$ when $s \to -\infty$. One may say that asymptotically the singular structures of $\hat{V}$ and $\hat{W}$ disappear exponentially and play merely a sub-dominant role.

Let us illustrate this issue by a representative example. The function

$$\hat{h}(s) = \sum_{k=1}^{\infty} \frac{2^{-k}}{s+k} = \frac{1}{2}\Phi\left(\frac{1}{2}, 1, 1+s\right), \tag{116}$$

where Φ is the so-called Lerch transcendent (see e.g. [37]), resembles the property of $\hat{V}$ of having infinitely many first-order poles accumulating at infinity with rapidly decreasing residuals. We have $\hat{h} \to 0$ for $|s| \to \infty, |\arg(s)| < \pi$. Let us now discuss the Bromwich integral (see (15), (16) and Fig. 2) which yields the associated inverse Laplace transform h:

$$h(\tau) = \mathcal{L}^{-1}[\hat{h}(s)](\tau) = \frac{1}{2\pi i}\int_{\Gamma_1} \hat{h}(s)e^{s\tau}ds. \tag{117}$$

The inverse Laplace transformation can be applied separately to each addend in (116), giving thus

$$h(\tau) = \sum_{k=1}^{\infty} 2^{-k}e^{-k\tau} = \frac{1}{2e^{\tau} - 1}, \tag{118}$$

which is just the sum of the residues of $\hat{h}(s)e^{s\tau}$ in the left half-plane:

$$\sum_{k=1}^{\infty} \mathrm{Res}_{-k}[\hat{h}(s)e^{s\tau}] = \sum_{k=1}^{\infty} 2^{-k}e^{-k\tau} = \frac{1}{2e^{\tau} - 1}. \tag{119}$$

[13]Outside this sector, in particular for $|\arg(s)| < \pi/2$, $|\hat{W}|$ tends to zero when $|s| \to \infty$, and hence the Bromwich integral (15) exists.

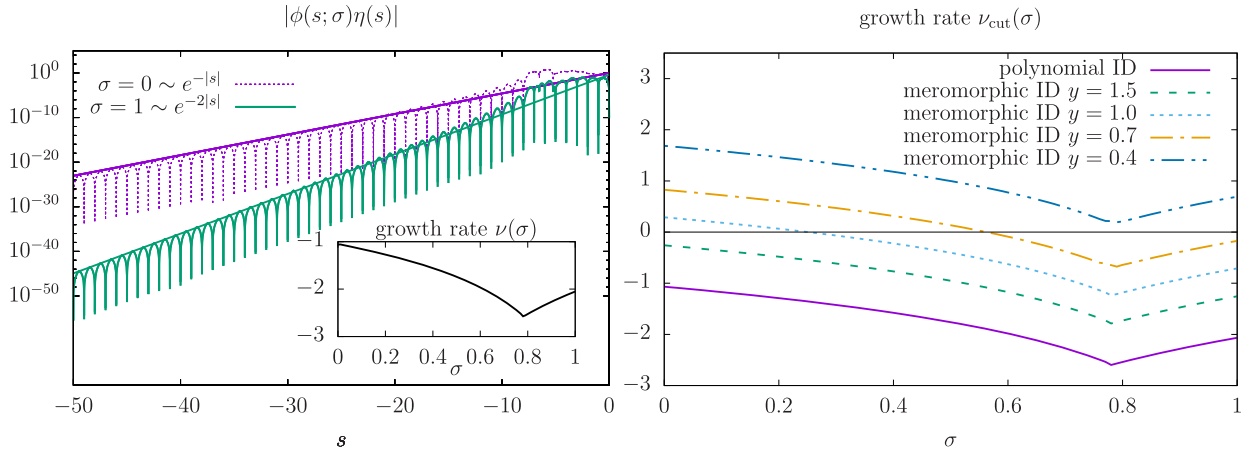

FIG. 9. Jump $\eta_n\phi_n(\sigma)$ of the Laplace transform $\hat{V}(\sigma;s)$ along the negative axis $s \in \mathbb{R}^-$ with prescribed parameters $\lambda = l = 0$. Left panel: for polynomial initial data $V_0(\sigma) = \sigma^2(1-\sigma)^4$, $\dot{V}_0(\sigma) = 0$ the decay is shown for $\sigma = 0$ (at $\mathcal{I}^+$) and for $\sigma = 1$ (at the horizon). The inset brings the growth rate $\nu_{\rm cut}(\sigma)$ for all $\sigma \in [0,1]$. Right panel: comparison of the grow rate for polynomial initial data against meromorphic initial data with single poles in the complex σ plane. Here, $V_0(\sigma) = 2\Re[(\sigma-\sigma_0)^{-1}]$, $\dot{V}_0(\sigma) = 0$, with $\sigma_0 = 0.5 + iy$. We observe exactly the same behavior for the growth rate as in the quasinormal mode case (see Fig. 8), i.e., $\nu_{\rm QNM}(\sigma) = \nu_{\rm cut}(\sigma)$.

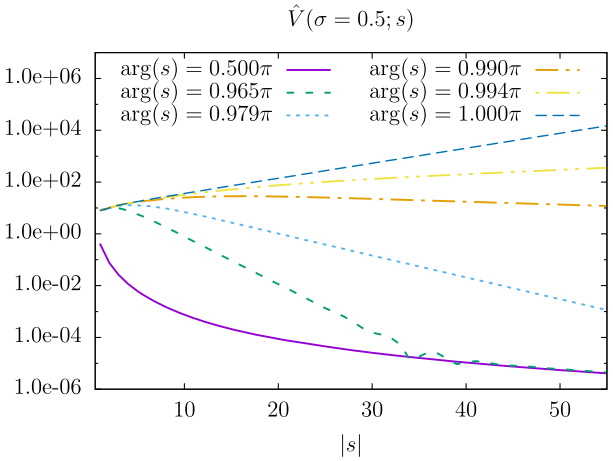

FIG. 10. Behavior of the Laplace transform $\hat{V}$ at the spatial location $\sigma = 0.5$ in the half-plane $\Re(s) < 0$ for meromorphic initial data $V_0(\sigma) = 2\Re[(\sigma-\sigma_0)^{-1}]$, $\dot{V}_0(\sigma) = 0$ with $\sigma_0 = 0.5 + i0.7$. It becomes apparent that $\hat{V}$ grows exponentially for $|\arg(s)| > 0.99\pi$. The strongest divergence is obtained for $|\arg(s)| = \pi$ and coincides there with the growth rate ν (here, $\nu \approx 0.13$).

It follows that

$$\frac{1}{2\pi i}\int_{\Gamma_2} \hat{h}(s)e^{s\tau}ds = \frac{1}{2\pi i}\int_{\Gamma_1} \hat{h}(s)e^{s\tau}ds = \sum_{k=1}^{\infty} \mathrm{Res}_{-k}[\hat{h}(s)e^{s\tau}],$$

i.e. the integral over the semicircular portion of Γ_2 vanishes in the limit of infinite radius. That is to say that Jordan's lemma applies, even though the function $\hat{h}$ possesses poles accumulating at infinity (and therefore does not satisfy the prerequisites required for a strict application of Jordan's lemma).

From the preceding considerations, we find that for $\nu < 0$ the integral over the semicircular portion of Γ_2 in the complex s plane vanishes. In contrast, for $\nu > 0$ the exponential divergence in the circular sector $|\arg(s)| > \frac{\pi}{2} + \arg(\nu + i\omega)$ ruins the applicability of Jordan's lemma. However, for times $\tau > \nu$ the functions $\hat{V}(\sigma;s)e^{s\tau}$ as well as $\hat{W}(s)e^{s\tau}$ possess the desired fall-off at infinity. This results from the fact that the strongest divergence in the circular sector is given by $e^{|s|\nu}$ in the limit $|\arg(s)| \to \pi$. We thus may finally conclude that the integral over the semicircular portion of Γ_2 does not contribute for (i) $\tau > 0$ when $\nu < 0$, and (ii) $\tau > \nu$ when $\nu > 0$.

V. SPECTRAL DECOMPOSITION

It is now an easy task to put the pieces together that we collected in the previous sections. The starting point is the representation (15) of the wave field V. If we deform the Bromwich integration path from Γ_1 to Γ_2 (see Fig. 2), we gather

(1) QNM contributions: Writing according to (60), (96), (102) and (28) the Laplace transform $\hat{V}$ in the vicinity of the QNM s_n as

$$\hat{V}(\sigma;s) = \frac{\eta_n\phi_n(\sigma)}{s - s_n} + \sum_{k=0}^{\infty} g_k(s)(1-\sigma)^k \qquad (120)$$

with coefficients $g_k(s)$ that are analytic in the vicinity of s_n (cf. discussion in Sec. IV E), we find

$$\frac{1}{2\pi i}\sum_{n=0}^{\infty}\oint_{C_n} \hat{V}(\sigma;s)e^{\tau s}ds = \sum_{n=0}^{\infty}\eta_n\phi_n(\sigma)e^{\tau s_n}, \qquad (121)$$

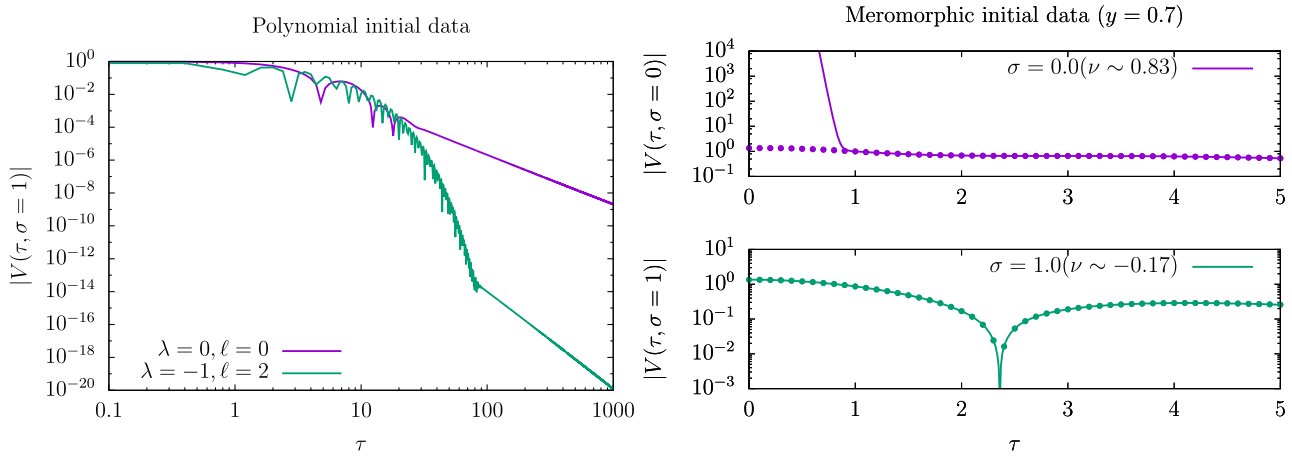

FIG. 11. Time evolution of the field $V(\tau,\sigma)$ according to the spectral decomposition (123). Left panel: polynomial initial data with $V_0(\sigma)=1$, $\dot{V}_0(\sigma)=0$, for $\lambda=0$, $\ell=0$ and -1, $\ell=2$. The spectral decomposition provides an efficient and stable method for a long time evolution (to be compared with the inverse Laplace transformation method in fig. 5). Right panel: meromorphic initial data $V_0(\sigma)=2\Re[(\sigma-\sigma_0)^{-1}]$, $\dot{V}_0(\sigma)=0$, with $\sigma_0=0.5+i0.7$ and $\lambda=0$, $\ell=0$. The continuous lines correspond to an evolution according to (123) while the dots are the results of the explicit time evolution with the code [34]. The spectral decomposition (123) is valid for time $\tau\gtrsim\nu(\sigma)$.

where C_n denotes a sufficiently small circle which encompasses in a counterclockwise fashion the QNM s_n (and only this one) and does not touch or cross the negative real s axis.

(2) The branch cut contribution amounts to

$$\begin{aligned}&\frac{1}{2\pi i}\int_{-\infty}^{0}[\hat{V}^{-}(\sigma;s)-\hat{V}^{+}(\sigma;s)]e^{\tau s}ds\\&=-\frac{1}{\pi}\int_{-\infty}^{0}\Im[\hat{V}^{+}(\sigma;s)]e^{\tau s}ds\\&=\int_{-\infty}^{0}\eta(s)\phi(\sigma;s)e^{\tau s}ds,\end{aligned}$$

where the integral is to be performed along the negative real s axis.

(3) No contribution from the semicircle for (i) $\tau>0$ when $\nu<0$, and (ii) $\tau>\nu$ when $\nu>0$, see discussion in Sec. IV G. We recall that ν resembles the mutual growth rate of QNM and branch cut amplitudes, cf. (107) and (110), obtained for analytic initial data.

In sum, we arrive at the following spectral decomposition of the wave field satisfying the dissipative wave equation (9):

$$V(\tau,\sigma)=\sum_{n=0}^{\infty}\eta_n\phi_n(\sigma)e^{\tau s_n}+\int_{-\infty}^{0}\eta(s)\phi(\sigma;s)e^{\tau s}ds. \tag{122}$$

We recap that $\{s_n\}$ are the QNMs of our wave equation in question. The functions $\phi_n(\sigma)$ and $\phi(\sigma;s)$ are the solutions to the homogeneous equation (27) taken at the QNMs and the branch cut $s\in\mathbb{R}^{-}$, respectively. The initial data are analytic for all $\sigma\in[0,1]$ and imply corresponding QNM amplitudes $\{\eta_n\}$ and the branch cut amplitude $\eta(s)|_{s\in\mathbb{R}^{-}}$ with characteristic mutual growth rate $\nu=\nu(\sigma)$. For $\nu<0$, the formula (122) was derived from the Bromwich integral for coordinate times $\tau>0$. However, having established (122), we see that the expressions actually make sense for any $\tau>\nu$, meaning that we may analytically expand the solution to such times. In sum, we may conclude that (122) is a valid representation of the wave field solution for all times $\tau>\nu(\sigma)$.

A reformulated version is given by

$$V(\tau,\sigma)=2\sum_{n=0}^{\infty}\Re(\eta_n\phi_n(\sigma)e^{\tau s_n})+\int_{-\infty}^{0}\eta(s)\phi(\sigma;s)e^{\tau s}ds, \tag{123}$$

where we utilized the condition (11) that allows us to count merely the quasinormal modes s_n with $\Im(s_n)>0$, as in Fig. 2. If algebraically special QNMs need to be taken into account, then the formula gets slightly modified; see Appendix D, Eq. (D10) therein.

Figure 11 displays the time evolution according to the spectral decomposition (123) for the two types of initial data discussed in this work. The left panel brings the results of a polynomial initial data $V_0(\sigma)=1$, $\dot{V}_0(\sigma)=0$ and, in order to compare with the results from Fig. 5 with chose $\lambda=0$, $\ell=0$ and -1, $\ell=2$. Moreover, the right panel compares the evolution according to (123) with the dynamics obtained numerically with the fully spectral code [34] for the meromorphic initial data $V_0(\sigma)=2\Re[(\sigma-\sigma_0)^{-1}]$, $\dot{V}_0(\sigma)=0$ ($\sigma_0=0.5+iy$) and $\lambda=0$, $\ell=0$. According to the growth rate $\nu(\sigma)$ showed

in the previous figs. 8 and 9, for $y = 0.7$, the spectral decomposition is valid only for $\tau \gtrsim 0.83$ at $\mathcal{I}^+$ ($\sigma = 0$), whereas Eq. (123) is valid for all time $\tau \gtrsim -0.17$ (in particular $\tau \geq 0$) at the horizon ($\sigma = 1$).

All in all, we have found that the formula (123) describes the wave field for all times $\tau > \nu(\sigma)$ and is, in contrast to the Bromwich integral method presented in Sec. IV C and Appendix A, particularly well suited to resolve highly accurately the late time tail behavior. More concretely, if τ is very large, then only the amplitude $\eta(s)$ within a tiny vicinity of the origin $s = 0$ in the complex s plane is important. Although the computation gets harder as $s \to 0$ [note that the coefficients μ_j diverge in this limit, cf. (48) and (50)], $\eta(s)$ can be computed independently for each s directly from the initial data. This is a striking advantage compared to a time evolution code for which the tail behavior results from a successive marching forward in time and depends therefore on all steps computed previously. A sophisticated study of tails in the more general Kerr spacetime is planned to be presented in a forthcoming article.

VI. DISCUSSION

In this article, we have numerically constructed the ingredients $\{s_n, \phi_n, \eta_n\}_{n=1}^{\infty}$ as well as $\{\phi(s), \eta(s)\}_{s\in\mathbb{R}^-}$ of the spectral decomposition (123) that describes solutions V to the initial value problem of the dissipative wave equation (9) with initial data that are analytic in terms of the compactified spatial hyperboloidal coordinate $\sigma \in [0, 1]$. The spectral form (123) arises through the study of the corresponding Laplace-transformed equation and an appropriate deformation of the associated Bromwich integration path. The ingredients in question were established in a sophisticated analysis of Taylor coefficients of relevant functions appearing in this context.

In the course of the aforementioned steps, we have discussed in detail that the characterization of QNMs in terms of the vanishing of the Wronskian determinant formed of specifically normalized solutions to the homogeneous Laplace transformed equation as described in [13] implies severe technical problems when attempting a straight-forward numerical computation.

In contrast, a well-functioning definition, which provides the justification of Leaver's continued fraction method [16] to determine the QNMs, is given through the vanishing of an appropriate discrete Wronskian determinant.

The form (123) has been numerically confirmed in a number of tests in which a selection of different analytical initial data were chosen. After the determination of $\{s_n, \phi_n, \eta_n\}_{n=1}^{\infty}$ and $\{\phi(s), \eta(s)\}_{s\in\mathbb{R}^-}$, formula (123) represents the desired solution for all coordinate times τ for which (123) makes sense, that is for $\tau > \nu(\sigma)$ where $\nu(\sigma)$ is the mutual growth rate of QNM and branch cut excitation coefficients. The test was performed through a comparison with the fully-pseudo spectral time evolution algorithm described in [34].

Before moving on, we elaborate on striking similarities with a specific dissipative wave equation on hyperbolic slices in Minkowski space that can be handled explicitly.

A. A dissipative wave equation with obstacle in Minkowski space

The following example is often being used in the so-called Lax-Phillips scattering theory [38]. Here, we aim not at a discussion within that framework but rather investigate the equation along the lines developed in this article.

Consider the ordinary wave equation on Minkowski space,

$$\frac{\partial^2 U}{\partial x^2} + \frac{\partial^2 U}{\partial y^2} + \frac{\partial^2 U}{\partial z^2} - \frac{\partial^2 U}{\partial t^2} = 0,$$

written in the Cartesian coordinates (x, y, z, t) of some inertial frame. We introduce the specific hyperbolic coordinates $(\varrho, \theta, \varphi, u)$ given through

$$\begin{aligned} x &= r_{\mathrm{O}}(\varrho + 1)\sin\theta\cos\varphi \\ y &= r_{\mathrm{O}}(\varrho + 1)\sin\theta\sin\varphi \\ z &= r_{\mathrm{O}}(\varrho + 1)\cos\theta \\ t &= r_{\mathrm{O}}(2u + \varrho + 1), \end{aligned}$$

where r_{O} denotes the coordinate radius of a given spherical obstacle at which we require the wave field U to vanish at all times. Assuming that U also vanishes at $\mathcal{I}^+$ (described by $\varrho \to \infty$), we rewrite it as

$$V(u, \varrho, \theta, \phi) = (\varrho + 1)U(u, \varrho, \theta, \phi)$$

and expand the auxiliary field $V(u, \varrho, \theta, \phi)$ into the spherical harmonics $Y_{\ell m}(\theta, \varphi)$ basis,

$$V(u, \varrho, \theta, \phi) = \sum_{\ell=0}^{\infty} \sum_{m=-\ell}^{\ell} V_{\ell m}(u, \varrho) Y_{\ell m}(\theta, \varphi).$$

We thus obtain a specific wave equation for each mode $V_{\ell m}(u, \varrho)$ (again we omit the indices ℓm from now on):

$$V_{,\varrho\varrho} - V_{,u\varrho} - \frac{l(l+1)}{(\varrho+1)^2} V = 0, \qquad V(u, \varrho = 0) = 0. \tag{124}$$

The second equation represents the boundary condition that the wave field be always zero at the obstacle. We consider (124) specifically for $l = 0$, and with the initial data $V(0, \varrho) = V_0(\varrho)$ the solution

$$V(u, \varrho) = V_0(\varrho + u) - V_0(u) \tag{125}$$

arises.

We now formulate the following question: For which initial data V_0 can the solution (125) be written in the form (123)? The answer is given by the inverse Laplace transform applied to $(V_0 - V_0|_{\varrho\to\infty})$ in terms of the spatial coordinate ϱ. In fact, if V_0 can be written as

$$V_0(\varrho) = \int_{-\infty}^{0} \eta(s)(e^{\varrho s} - 1)ds = \mathcal{L}\{\eta(-s)\}(\varrho) + V_\infty,$$
$$V_\infty = V_0|_{\varrho\to\infty} = -\int_{-\infty}^{0} \eta(s)ds \tag{126}$$

for some function $\eta(s)$, then (125) turns into

$$V(u,\varrho) = \int_{-\infty}^{0} \eta(s)\underbrace{(e^{\varrho s} - 1)}_{=\phi(\varrho;s)}e^{su}ds; \tag{127}$$

i.e., we obtain the form (123) with a purely continuous part. Now, if we expand V_0 into the entire complex ϱ plane and find some finite value,

$$\varrho_{\max} := \max\{\Re(\varrho_S) : \varrho_S \text{ is singularity of } V_0\}, \tag{128}$$

i.e. all singularities of V_0 are located to the left of the line $\Re(\varrho) = \varrho_{\max}$, then we have for $s \to -\infty$:

$$|\eta(s)| = |\mathcal{L}^{-1}\{V_0(\varrho) - V_\infty\}(-s)| \sim e^{-s\varrho_{\max}}. \tag{129}$$

We thus conclude: The spectral decomposition (127) holds for $u > \varrho_{\max}$ if the complex continuation of the initial data $V_0(\varrho)$ onto the complex ϱ plane reveals singular structures located entirely to the left of the line $\Re(\varrho) = \varrho_{\max}$ away from infinity.

This is a very similar situation as the one that we encountered in the Schwarzschild case. In this Minkowski example, however, we can identify an explicit relation between the spatially constant growth rate and the location of singular structures of the initial data $V_0(\varrho)$, namely $\nu = \varrho_{\max}$.

Going further and considering now singularities located at infinity in the complex ϱ plane, we find that the matter gets more subtle. The following examples provide an impression (take α, $\omega \in \mathbb{R}^+$ in the examples 2 and 4):

No.	$V_0(\varrho)$	$\eta(s)$
1	$e^{-\varrho} - 1$	$\delta(s+1)$
2	$e^{-\alpha\varrho}\sin(\omega\varrho)$	nonexistent
3	$e^{-\sqrt{\varrho+1}} - 1$	$\frac{e^{s+1/(4s)}}{2\sqrt{\pi}(-s)^{3/2}}$
4	$(\varrho+1)^{-\alpha} - 1$	$\frac{e^s(-s)^{\alpha-1}}{\Gamma(\alpha)}$

(130)

The first example describes a purely exponential falloff of the solution, while the second one is a ring down oscillation with arbitrarily chosen frequency ω and decay rate α.

If we discuss the several choices V_0 in terms of a compactified spatial coordinate $\sigma = 1/(\varrho+1)$, then we find for the first three examples in (130) that the corresponding $V_0(\sigma)$ is C^∞ at $\sigma = 0$. In the fourth example, however, we have $V_0(\sigma) = \sigma^\alpha - 1$ which, for $\alpha < 1$, is not differentiable at $\sigma = 0$. We conclude that C^k-regularity, and in particular C^∞-smoothness of the initial data $V_0(\sigma)$ at $\sigma = 0$, is neither sufficient nor necessary for the existence of a corresponding function $\eta(s)$. This point deserves further clarification, to be conducted elsewhere.

B. Conclusion and outlook

The final result of our analytical considerations combined with numerous numerical examples can be formulated as the following conjecture:

Given analytical initial data $V_0(\sigma)$ and $\dot{V}_0(\sigma)$ for the wave equation (9). Then the spectral decomposition (123) holds for all $\tau > \nu(\sigma)$ where $\nu(\sigma)$ is the mutual growth rate of quasinormal mode and branch cut excitation coefficients defined by (107) and (110).

A strict mathematical proof of this conjecture remains a challenging task which is far outside the scope of this paper.

Clearly, it would be desirable to relax the conditions imposed on the initial data to allow for more generic configurations (for instance, data with compact support). From our experiences gathered in this paper as well as through numerous dynamical computations performed by many authors we surmise that the conjecture would still hold for generic initial data that are analytic in a vicinity of $\sigma = 0$, i.e. at $\mathcal{I}^+$. More precisely, we expect that there are for each such initial data individual QNM as well as branch cut amplitudes with characteristic growth rates $\nu_{\mathrm{QNM}}(\sigma)$ and $\nu_{\mathrm{cut}}(\sigma)$ (maybe different for nonanalytical data) such that the spectral decomposition (123) holds for all $\tau > \nu(\sigma)$ where $\nu(\sigma) = \max\{\nu_{\mathrm{QNM}}(\sigma), \nu_{\mathrm{cut}}(\sigma)\}$. These amplitudes, however, cannot be determined by the methods described in this paper, as they rely on an analysis of Taylor expansions. Note that we had to exclude initial data that are not analytic at $\mathcal{I}^+$. Again a look at the dissipative wave equation in Minkowski space illuminates the situation, specifically example 2 in table (130) for which a branch cut amplitude and hence a corresponding growth rate does not exist. Consequently, for such initial data the spectral decomposition never holds. Going back to the Schwarzschild case, we expect that likewise for generic initial data of the form (39) we cannot identify QNM and branch cut amplitudes, i.e., (123) never holds ($\nu = \infty$), unless the Laplace parameter in (39) is chosen to be some QNM, $s = s_n$, in which case (123) holds for all times τ ($\nu = -\infty$).

At the end, a final remark seems to be in place. In [24], it has been argued that "the integral over the quarter circles at infinite frequency produces the early time response of the black hole." Similar comments can be found in other papers (see e.g. [39]), and they all seem to be reformulated versions of Leaver's statement from [18], "It is G_F that

propagates the high-frequency response, and which reduces to the free-space Green's function in the limit as the mass of the black hole goes to zero." Our considerations lead us, however, to a different interpretation. We have seen that, for generic analytical initial data, the Laplace transform $\hat{V}$ diverges exponentially in some circular sector $|\arg(s)| \in (\pi-\varepsilon,\pi)$ in the complex s plane when $|s|\to\infty$. This means, that the integral over the quarter circles at infinite frequency mentioned before cannot be evaluated. However, in the course of time, concretely for $\tau > \nu(\sigma)$, the associated $\hat{V}$ for initial data taken on such time slices vanishes when $|s|\to\infty$, $|\arg(s)|<\pi$, and hence the integral in question does not contribute by virtue of Jordan's lemma. Therefore, we encounter the impression that the proposed early time contribution of the integral over the quarter circles at infinity is a misinterpretation. This integral cannot be evaluated for small times (and thus cannot reasonably be discussed physically) and vanishes for data at larger times $\tau > \nu(\sigma)$.

We conclude this article with the observation that, due to our experiences gathered in the Minkowski example, the case in which the singularity is located at $\mathcal{I}^+$, i.e. at $\sigma = 0$, is expected to require a more sophisticated investigation. While it might appear as a minor remaining uncertainty, this issue plays a fundamental role when attempting to identify an appropriate linear operator acting on an associated function space, whose spectrum is $\{s_n\}\cup\mathbb{R}^-$ with corresponding proper and improper eigenvectors ϕ_n and $\phi(s)$. Again, the treatment of this interesting functional-analytical question is far beyond the scope of this paper.

ACKNOWLEDGMENTS

The authors are deeply indebted to Bernd Schmidt for bringing our attention to this interesting topic and for numerous insightful discussions. This work was supported by the DFG Grants No. SFB/Transregio 7 Gravitational Wave Astronomy and No. GRK 1523/2. Rodrigo P. Macedo was supported by the CNPq under the Ciência sem Fronteiras program.

APPENDIX A: THE BROMWICH INTEGRAL

The Bromwich integral solution method considers the integration path Γ_1 [see (16)], that is, values $\hat{V}(s)$ for $s = \xi + i\chi$ with some prescribed $\xi > 0$ and $\chi \in (-\infty,\infty)$ are collected in order to evaluate (2), i.e.

$$V(\tau,\sigma) = \frac{e^{\xi\tau}}{2\pi}\int_{-\infty}^{+\infty}\hat{V}(\sigma;\xi+i\chi)e^{i\chi\tau}d\chi. \tag{A1}$$

Since $V(\tau,\sigma)$ is bounded, its Laplace transform $\hat{V}$ vanishes for $|s|\to\infty$, $\arg(s)\in(-\pi/2,\pi/2)$; see (10). Consequently, we have for all s with $\Re(s)>0$, via Jordan's lemma,

$$\lim_{R\to\infty}\int_{C_R(s)}\frac{\hat{V}(\sigma;\tilde{s})d\tilde{s}}{\tilde{s}-s} = 0, \tag{A2}$$

where $C_R(s)$ is a semicircle in the right half-plane about the point s, i.e.

$$C_R(s) = \{\tilde{s}\in\mathbb{C}|\tilde{s} = s + \mathrm{Re}^{if}, f\in(-\pi/2,\pi/2)\}.$$

Consider now Cauchy's integral theorem,

$$P\oint_{\Gamma_R(s)}\frac{\hat{V}(\sigma;\tilde{s})ds}{\tilde{s}-s} = \pi i\hat{V}(\sigma;s), \tag{A3}$$

where

$$\Gamma_R(s) = C_R(s)\cup\{\tilde{s}\in\mathbb{C}|\tilde{s} = s + i\tilde{\chi},\tilde{\chi}\in(-R,R)\},$$

with P denoting the Cauchy principal value and the integration evaluated in a counterclockwise fashion along the closed curve $\Gamma_R(s)$. By virtue of (A2) and (A3), it follows that the imaginary part of $\hat{V}$ is the Hilbert transform of the real part:

$$\Im[\hat{V}(\sigma;\xi+i\chi)] = \frac{1}{\pi}P\int_{-\infty}^{\infty}\frac{\Re[\hat{V}(\sigma;\xi+i\bar{\chi})]d\bar{\chi}}{\bar{\chi}-\chi}. \tag{A4}$$

We insert this expression into (A1) and obtain via

$$P\int_{-\infty}^{\infty}\frac{e^{-i\omega}}{\omega}d\omega = -\pi i$$

that

$$\begin{aligned}V(\tau,\sigma) &= \frac{e^{\xi\tau}}{\pi}\int_{-\infty}^{+\infty}\Re[\hat{V}(\sigma;\xi+i\chi)]e^{i\chi\tau}d\chi\\ &= \frac{2e^{\xi\tau}}{\pi}\int_0^{\infty}\Re[\hat{V}(\sigma;\xi+i\chi)]\cos(\chi\tau)d\chi,\end{aligned} \tag{A5}$$

where the latter expression arises through the symmetry condition (11). Now, for some prescribed auxiliary parameter $s_{\mathrm{P}}\in\mathbb{R}_0^-$, we compactify the integration interval with the help of the new variable $x\in(0,x_{\mathrm{P}}]$ via

$$x = \frac{x_{\mathrm{P}}}{1+x_{\mathrm{P}}\chi^2}\quad\text{where } x_{\mathrm{P}} = (\xi-s_{\mathrm{P}})^{-2}. \tag{A6}$$

Taking into account that $\Re(\hat{V})$ is an even function in the variable χ and vanishes when $\chi\to\infty$, we may approximate $x^{-1}\Re(\hat{V})$ in terms of a Chebyshev series:

$$\Re[\hat{V}(\sigma;\xi+i\chi)]\approx x\sum_{j=0}^{n_\chi-1}c_j(\sigma;\xi,s_{\mathrm{P}})T_j\left(\frac{2x}{x_{\mathrm{P}}}-1\right), \tag{A7}$$

where a particular numerical resolution n_χ was chosen. The Chebyshev coefficients $c_j(\sigma;\xi,s_{\mathrm{P}})$ are obtained through

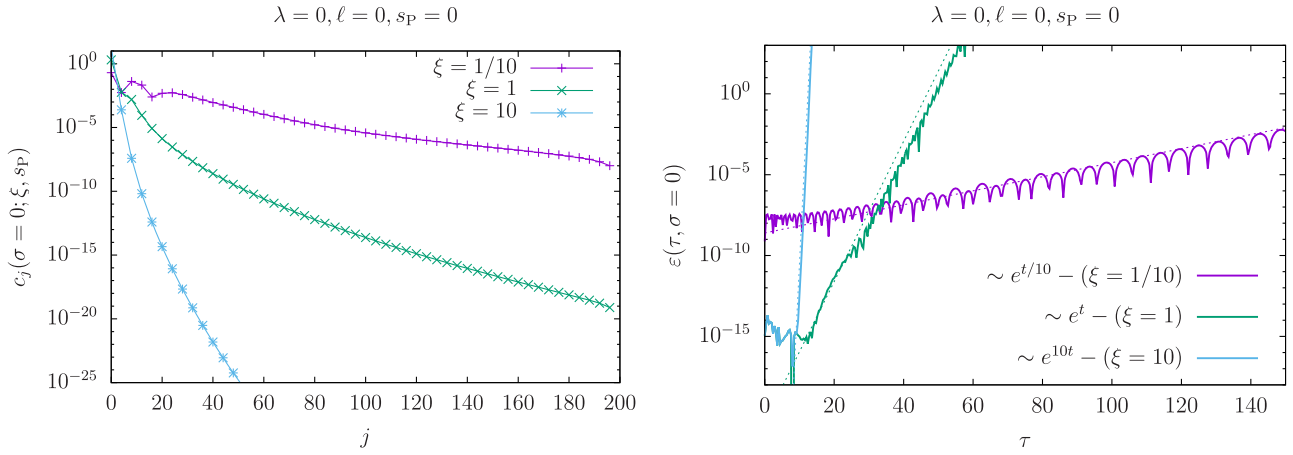

FIG. 12. Numerical accuracy of the Bromwich integral method with resolution $n_\chi = 200$, applied to the initial data $V_0(\sigma) = 1$, $\dot{V}_0(\sigma) = 0$, with parameter $s_P = 0$ [cf. (A6)] along the Bromwich integration paths $\Re(s) = \xi \in \{1/10, 1, 10\}$. Left panel: Chebyshev coefficients $c_j(0; \xi, s_P)$, cf. (A7) and their dependence on ξ. Right panel: Corresponding dynamical error $\varepsilon(\tau, \sigma = 0)$ which diverges as $e^{\xi\tau}$. Results were obtained with the fixed Taylor resolutions $k_{\max} = 500$, $J_{\max} = 10$, cf. Sec. IV.

requiring equality in (A7) at the Chebyshev-Gauss grid points

$$\chi_k = \sqrt{\frac{1}{x_k} - \frac{1}{x_P}}, \quad \text{with} \quad x_k = x_P \cos\left(\frac{\pi(2k+1)}{2n_\chi}\right)$$

and $k = 0, \ldots, n_\chi - 1$. Here, the left-hand sides in (A7) are evaluated according to the procedure described in Sec. IV. Note that $x^{-1}\Re(\hat{V})$ is C^∞ for $x \in [0, x_P]$,[14] and hence a Chebyshev expansion provides an accurate numerical approximation.

Considering the polynomial structure of the T_j's explicitly, we introduce coefficients $\mathcal{P}_{jl}$ via the requirements

$$xT_j\left(\frac{2x}{x_P} - 1\right) = \sum_{l=0}^{j} \mathcal{P}_{jl} x^{l+1}. \tag{A8}$$

Through this rearrangement we can explicitly evaluate the integral (A5):

$$V(\tau, \sigma) \approx \sum_{j=0}^{n_\chi - 1} c_j(\sigma; \xi, s_P) \sum_{l=0}^{j} \mathcal{P}_{jl} Q_l(\tau; \xi, s_P) \tag{A9}$$

with

$$\begin{aligned} Q_l(\tau; \xi, s_P) &= \frac{2e^{\xi\tau}}{\pi} \int_0^{+\infty} x^{l+1} \cos(\chi\tau) d\chi \\ &= \frac{2e^{s_P\tau}}{l!} \sum_{k=0}^{l} \frac{(l+k)!}{(l-k)!k!} [2(\xi - s_P)]^{-(l+k+1)} \tau^{l-k}. \end{aligned} \tag{A10}$$

[14]Analyticity breaks down at $x = 0$ when $\chi \to \infty$; see discussion in Sec. IV G.

We provide a few examples of the functions $Q_l(\tau; \xi, s_P)$:

$$\begin{aligned} Q_0(\tau; \xi, s_P) &= \frac{e^{s_P\tau}}{\xi - s_P} \\ Q_1(\tau; \xi, s_P) &= e^{s_P\tau} \frac{1 + \tau(\xi - s_P)}{2(\xi - s_P)^3} \\ Q_2(\tau; \xi, s_P) &= e^{s_P\tau} \frac{3 + 3\tau(\xi - s_P) + \tau^2(\xi - s_P)^2}{8(\xi - s_P)^5} \end{aligned}$$

The systematic error of this method is a consequence of the truncation of the Chebyshev series (A7) at the resolution order n_χ. For $\tau \sim 0$, the accuracy is determined by the behavior of the Chebyshev coefficients $c_j(\sigma; \xi, s_P)$, whereas the time propagation of this initial numerical error is related to the behavior of the functions $Q_l(\tau; \xi, s_P)$. As a representative we consider the coordinate location $\sigma = 0$ and study how the choice of the two parameters $\xi > 0$ and $s_P \leq 0$ affects the numerical performance.

Figure 12 compares the dependency of $c_j(0; \xi, s_P)$ on the parameter ξ (left panel) for a fixed value $s_P = 0$. Note that the coefficients fall off stronger and stronger as ξ increases. However, the right panel of this figure reveals that the dynamical error grows in the course of time exponentially as $e^{\xi\tau}$.[15]

For $\xi \sim 0$, we can improve the efficiency of the method by shifting the parameter s_P accordingly. Fixing now $\xi = 1/10$, the left panel of Fig. 13 depicts $c_j(0; \xi, s_P)$

[15]The dynamical error is defined as $\varepsilon(\tau, \sigma) = |V_{\text{Bromwich}}(\tau, \sigma) - V_{\text{HighAcc}}(\tau, \sigma)|$, where $V_{\text{Bromwich}}(\tau, \sigma)$ is the solution obtained via the Bromwich integral method and $V_{\text{HighAcc}}(\tau, \sigma)$ being a highly accurate numerical solution obtained with a time-marching scheme based on a fully spectral code [34].

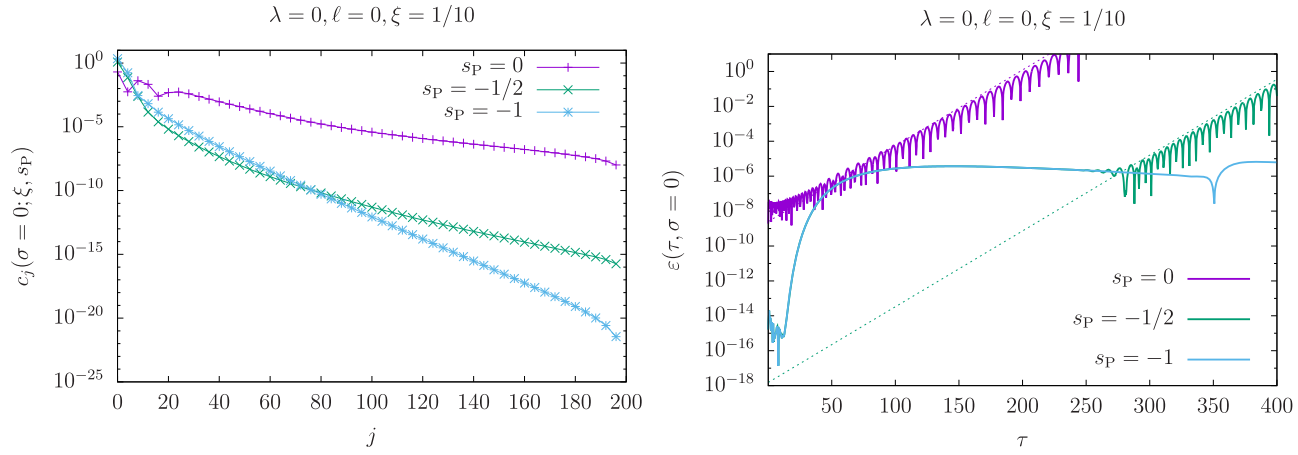

FIG. 13. Numerical accuracy of the Bromwich integral method with resolution $n_\chi = 200$, as in Fig. 12 applied to the initial data $V_0(\sigma) = 1$, $\dot{V}_0(\sigma) = 0$, along the fixed Bromwich integration path $\Re(s) = \xi = 1/10$ for different parameters s_P [cf. (A6)]. Left panel: Chebyshev coefficients $c_j(0; \xi, s_P)$, cf. (A7) and their dependence on s_P. Right panel: Corresponding dynamical error $\varepsilon(\tau, \sigma = 0)$. Results were obtained with the fixed Taylor resolutions $k_{\max} = 500$, $J_{\max} = 10$, cf. Sec. IV.

for different values of s_P. Note that an appropriate choice of s_P significantly enhances the decay rate of $c_j(0; \xi, s_P)$. As in Fig. 12, the right panel of Fig. 13 displays the corresponding dynamical errors, and it becomes apparent that a stable solution can be obtained for a much longer time period. In the long run, however, the time behavior of the numerical Bromwich solution is dominated by the decay rate $\sim e^{s_P \tau} \tau^l$ of the integral terms $Q_l(\tau; \xi, s_P)$, cf. (A10) and Fig. 5. Consequently, for very late times, the dynamical error corresponds to the inverse power law behavior of the tail decay.

We conclude that in contrast to the spectral decomposition (123), the Bromwich integral method, as realized in this work, is not suitable for describing the wave field's long term tail behavior. It does, however, provide a neat test and justification of the Taylor coefficient techniques which present the core of this work.

APPENDIX B: EXAMPLES FOR RELEVANT TAYLOR ASYMPTOTICS

In this section, we provide an explicit example that resembles the properties of a function f,

$$f = \sum_{k=0}^{\infty} H_k (1 - \sigma)^k, \tag{B1}$$

whose Taylor coefficients posses an asymptotics of the kind given in (36) and (37). The explicit example is given by the function

$$f = e^{s/\sigma}. \tag{B2}$$

It can easily be verified that f satisfies the ordinary differential equation

$$[\sigma^2 \partial_\sigma + s] f = 0. \tag{B3}$$

Inserting the Taylor expansion (B1) into (B3) yields the recurrence relation

$$(k+1) H_{k+1} - (2k + s) H_k + (k-1) H_{k-1} = 0. \tag{B4}$$

Treating this recurrence relation in exactly the same manner as described in Sec. IV A, we obtain the following asymptotics of the Taylor coefficients:

$$H_k \sim \underbrace{A_\infty^\pm k^{-3/4} e^{\pm 2\sqrt{sk}} Y\left(\pm \frac{1}{\sqrt{k}}\right)}_{=: a_k^\pm}, \quad k \to \infty \tag{B5}$$

with

$$Y(x) = 1 + \sum_{j=1}^{\infty} y_j x^j, \tag{B6}$$

$$y_1 = \frac{4s^2 - 9}{48\sqrt{s}} \tag{B7}$$

$$y_2 = \frac{s^3}{288} - \frac{5s}{64} - \frac{15}{512s} \ldots \text{etc.} \tag{B8}$$

Clearly, for $s \notin \mathbb{R}^-$, the term in (B5) with the positive sign (meaning the square root in the exponent with positive real part) is dominant in comparison to the term with the negative sign. Hence we have:

$$A_\infty^+ = \lim_{k \to \infty} (H_k k^{3/4} e^{-2\sqrt{sk}}), \qquad s \notin \mathbb{R}^-. \tag{B9}$$

If we compute the coefficients H_k with the help of (B4), utilized here as upwards recurrence relation with $H_{-1} = 0$

and $H_0 = e^s$, we can determine the limit (B9) numerically. Examples are provided in (B12).

For $s \in \mathbb{R}^-$, however, both asymptotics in (B5) need to be considered. Then the two unknowns $A^\pm_\infty$ can be obtained through the conditions

$$H_1 = se^s, \qquad H_2 = \frac{s}{2}(2+s)e^s, \tag{B10}$$

which result from (B4) for $k = 1$ and $k = 0$, taking into account that $H_{-1} = 0$ and $H_0 = e^s$. Indeed, if we write in accordance with (B5)

$$H_k = A^+_\infty a^+_k + A^-_\infty a^-_k \tag{B11}$$

for two coefficients H_{K+1} and H_K, where K is some large number, and climb down to H_2 and H_1 utilizing (B4) now as downwards recurrence relation, the conditions (B10) determine uniquely the two unknowns $A^\pm_\infty$. We generally find that $A^+_\infty = (A^-_\infty)^* \propto e^{\pi i/4}$ for $s \in \mathbb{R}^-$; see examples in (B12).

$$\begin{aligned}
&s = 1\colon\ A^+_\infty \approx 0.46509\\
&s = e^{\pi i/4}\colon\ A^+_\infty \approx 0.34251 + 0.20995i\\
&s = i\colon\ A^+_\infty \approx 0.17696 + 0.21969i\\
&s = e^{3\pi i/4}\colon\ A^+_\infty \approx 0.11641 + 0.16027i\\
&s = -\frac{1}{2}\colon\ A^+_\infty \approx 0.13063 + 0.13063i\\
&s = -1\colon\ A^+_\infty \approx 0.12099 + 0.12099i\\
&s = -2\colon\ A^+_\infty \approx 0.08727 + 0.08727i\\
&s = -10\colon\ A^+_\infty \approx 0.00239 + 0.00239i
\end{aligned} \tag{B12}$$

The preceding detailed study provides us with an understanding of regularity properties of solutions $\phi(s)$ to the homogeneous equation

$$\mathbf{A}(s)\phi(s) = 0, \qquad \phi(s) \text{ analytic at } \sigma = 1, \tag{B13}$$

when s is not a quasinormal mode, $s \notin \{s_n\}$. Just like $f = e^{s/\sigma}$, the functions $\phi(s)$ diverge at $\sigma = 0$ if $\Re(s) > 0$. However, they are C^∞ for all $\sigma \in [0,1]$ if $\Re(s) < 0$, despite the fact that the corresponding Taylor coefficients' magnitudes $|H_k|$ grow faster in k than any polynomial (for $s \notin \mathbb{R}^-$). It is interesting to note that apparently the relation between the growth rate of $|H_k|$ and the frequency in the coefficients' oscillations determines whether the function is C^∞ or diverges at $\sigma = 0$:

$$\begin{aligned}
&\phi = \sum_{k=0}^{\infty} H_k(1-\sigma)^k,\\
&H_k \sim e^{(g+i\omega)\sqrt{k}} \text{ as } k \to \infty\colon g < |\omega|\colon\ \phi \text{ is } C^\infty,\\
&\quad g > |\omega|\colon\ \phi \text{ diverges.}
\end{aligned} \tag{B14}$$

As depicted in Sec. IV A, this has the consequence that for $\Re(s) < 0$ there are C^∞-initial data (39) which imply the regular C^∞-solution (40) to our wave equation (9). The situation is very similar to the Minkowskian wave obtained for the initial data No. 2 in (130). Note that for this example the spectral representation (127) does not hold, and hence we presume that likewise (123) is not applicable for the initial data (39); see discussion in Sec. VI B. The particular case $s \in \mathbb{R}^-$ provides us with a solution with an exponential fall-off without oscillations, to be compared with the Minkowskian wave associated with the initial data No. 1 in (130). Just like there, the situation can be described marginally with the formula (123) if we accept Dirac-delta-type amplitudes $\eta(s)$.

Let us now take a closer look at the function Φ introduced in (38) which satisfies the ODE

$$\begin{aligned}
0 = {}& \sigma^2(1-\sigma)\Phi'' + [(\lambda-1)\sigma(3\sigma-2) - s]\Phi'\\
&- [(\lambda-1)(2\lambda\sigma - \lambda - \sigma) + \ell(\ell+1)]\Phi.
\end{aligned} \tag{B15}$$

Writing Φ as f in (B1) in terms of a Taylor expansion about $\sigma = 1$, we find the recurrence relation

$$\alpha_k H_{k+1} + \tilde{\beta}_k H_k + \tilde{\gamma}_k H_{k-1} = 0 \tag{B16}$$

with

$$\begin{aligned}
&\tilde{\beta}_k = -\lambda^2 + 4k\lambda + 2\lambda - 2k(k+1) - \ell(\ell+1) - 1\\
&\tilde{\gamma}_k = (k - 2\lambda)(k - \lambda).
\end{aligned} \tag{B17}$$

The analysis of the relation (B16) along the lines presented in Sec. IV A reveals the asymptotics

$$H_k = U^+_\infty u^+_k + U^-_\infty u^-_k \tag{B18}$$

with

$$u^\pm_k \sim k^{-\frac{1}{4}(4\lambda+2s-3)} e^{\pm 2\sqrt{-sk}} Z\left(\pm\frac{1}{\sqrt{k}}\right), \qquad (k \to \infty), \tag{B19}$$

which by virtue of (B15) describes for $\Re(s) > 0$ a function Φ that is C^∞ for all $\sigma \in [0,1]$ but blows up exponentially at $\sigma = 0$ for $\Re(s) < 0$.

We conclude this section by providing an example resembling the properties of a function f with Taylor coefficients H_k which can be written as in (B11) with $A^+_\infty = 0$, i.e. with an asymptotics similar to the one described in (42). This example is meant to demonstrate the analytical properties of the solutions ϕ_n to the homogeneous problem (27) at the QNMs $s_n \notin \mathbb{Z}^-$.

Looking for some $j \in \mathbb{N}$ at the inhomogeneous equation

$$[\sigma^2\partial_\sigma + s]f = \sigma^j, \tag{B20}$$

where $s \in \mathbb{C}\backslash\mathbb{R}_0^-$, we find the solution

$$f(\sigma) = \sigma^{j-1} e^{s/\sigma} E_j\left(\frac{s}{\sigma}\right),$$

which is analytic for $\sigma \in (0,1]$ and still C^∞ at $\sigma = 0$. Its Taylor coefficients obey the asymptotics $H_k \sim A_\infty^- a_k^-$ as $k \to \infty$ [see (B5)]. Taking again this expression for two coefficients H_{K+1} and H_K, where K is some large number, and climbing down to H_j utilizing (B4) once more as downwards recurrence relation,[16] the condition $H_j = (-1)^j f^{(j)}(\sigma = 1)/j!$ implies the numerical value of A_∞^-. Exemplary cases for $j = 1$ are provided in (B21).

$$\begin{aligned} &s = 1\colon\ A_\infty^- \approx -2.92228 \\ &s = e^{\pi i/4}\colon\ A_\infty^- \approx -2.15206 - 1.31915i \\ &s = i\colon\ A_\infty^- \approx -1.11188 - 1.38033i \\ &s = e^{3\pi i/4}\colon\ A_\infty^- \approx -0.73143 - 1.00699i \end{aligned} \tag{B21}$$

APPENDIX C: NEGATIVE INTEGER LAPLACE PARAMETERS

When the Laplace parameters s is a negative integer then $\alpha_{-(s+1-\lambda)}$ as well as γ_{-s} and $\gamma_{-(s+\lambda)}$ vanish. Consequently, neither the forward recurrence relation (31) nor the backward recurrence relation (53) can be completely carried out for the sequences $\{H_k\}$ and $\{I_k\}$, respectively. Yet, the calculation of the jump function for values in the neighborhood of the negative integers indicates that the solution $\hat{V}(\sigma; s)$ is well behaved at $s \in \mathbb{Z}^-$.

Here we modify the calculation of the Taylor coefficients a_k [cf. (60)] for $s \in \mathbb{R}^-\backslash\mathbb{Z}^-$ and consider subsequently a smooth limit of s towards the neighboring negative integer.[17] To this end, we start by defining the critical indices

$$\begin{aligned} \tilde{k} &= \lfloor -s - 1 + \lambda \rceil, \\ \hat{k} &= \lfloor \min(-s, -s - \lambda) \rceil, \\ k^* &= \lfloor \max(-s, -s - \lambda) \rceil, \end{aligned} \tag{C1}$$

where $\lfloor \bullet \rceil$ denotes the round function which provides the nearest integer. We further introduce the new coefficients K_k and J_k via

$$K_k = \begin{cases} H_k & \text{for } k \le \tilde{k} \\ \alpha_{\tilde{k}} H_k & \text{for } k > \tilde{k} \end{cases}, \tag{C2}$$

$$J_k = \begin{cases} \gamma_{\hat{k}}\gamma_{k^*} I_k & \text{for } k < \hat{k} \\ \gamma_{k^*} I_k & \text{for } \hat{k} \le k < k^* \\ I_k & \text{for } k \ge k^* \end{cases}. \tag{C3}$$

Now, for $k < \tilde{k}$ and for $k > \tilde{k} + 1$, the coefficients K_k satisfy the same forward recurrence relation as H_k, cf. (31). Besides, combining the definition (C2) with the recurrence relation (31) for $k = \tilde{k}$ and $k = \tilde{k} + 1$ one gets

$$K_{\tilde{k}+1} = -(\beta_{\tilde{k}} K_{\tilde{k}} + \gamma_{\tilde{k}} K_{\tilde{k}-1}), \tag{C4}$$

$$K_{\tilde{k}+2} = -(\beta_{\tilde{k}} K_{\tilde{k}+1} + \alpha_{\tilde{k}}\gamma_{\tilde{k}} K_{\tilde{k}})/\alpha_{\tilde{k}+1}. \tag{C5}$$

In the limit $s \to \lfloor s \rceil \in \mathbb{Z}^-$, both $K_{\tilde{k}+1}$ and $K_{\tilde{k}+2}$ are well defined, despite the fact that $\alpha_{\tilde{k}} \to 0$. This can be followed from the relations (31), (C4) and (C5).

The analysis of the coefficients J_k follows a similar route. They satisfy the same backward recurrence relation (53) for the coefficients I_k, except for the values $k = k^*$, $k = k^* - 1$, $k = \hat{k}$ and $k = \hat{k} - 1$. Combining the definition (C3) with the backward recurrence relation (53) for $k = k^*$ and $k = k^* - 1$, we obtain

$$J_{k^*-1} = -(\alpha_{k^*} J_{k^*+1} + \beta_{k^*} J_{k^*}), \tag{C6}$$

$$J_{k^*-2} = -(\gamma_{k^*}\alpha_{k^*-1} J_{k^*} + \beta_{k^*-1} J_{k^*-1})/\gamma_{k^*-1}. \tag{C7}$$

Likewise, if we replace here k^* by $\hat{k}$, then we obtain expressions which provide $J_{\hat{k}-1}$ and $J_{\hat{k}-1}$.[18] Again, eqs. (C6) and (C7) (together with the corresponding case k^* replaced by $\hat{k}$) are well defined in the limit $s \to \lfloor s \rceil \in \mathbb{Z}^-$ where γ_{k^*} and $\gamma_{\hat{k}}$ tend to zero.

We now turn our attention to the computation of the coefficients a_k. Given a_0 we can invoke the forward recurrence relation (61) to compute a_k for $1 \le k \le \tilde{k}$. However, since $\alpha_{\tilde{k}} \to 0$ for $s \to \lfloor s \rceil$, the forward recurrence calculation of $a_{\tilde{k}+1}$ breaks down in this limit. Then for larger indices $k \ge \tilde{k} + 2$, the forward recurrence relation (61) can again be used. That is to say that for the computation of the entirety $\{a_k\}$ in the limit $s \to \lfloor s \rceil$ via the forward recurrence relation it is necessary to provide the two coefficients a_0 and $a_{\tilde{k}+1}$. Indeed, they can be obtained explicitly by rewriting Eq. (71) with the help of (C2) and (C3). In terms of the abbreviations

$$\tilde{\Pi}_j^{(\alpha)} = \prod_{m=0}^{j-1} \alpha_m \tag{C8}$$

[16] With the inhomogeneity σ^j in (B20), the recurrence relation (B4) remains the same for $k > j$.

[17] Throughout this section, we assume that the negative real axis is approached from above. For simplicity, we omit the index $\bullet^+$ in all the relevant quantities.

[18] Care must be taken if $|\lambda| = 1$, for then $k^* - 1 = \hat{k}$ and $k^* - 2 = \hat{k} - 1$.

$$\Pi_j^{(\alpha)} = \prod_{\substack{m=0 \\ \{m\neq\hat{k}\}}}^{j-1} \alpha_m \tag{C9}$$

$$\Pi_j^{(\gamma)} = \prod_{\substack{m=0 \\ \{m\neq k^*\} \\ \{m\neq\hat{k}\}}}^{j} \gamma_m, \tag{C10}$$

we find:

$$a_0 = -\frac{1}{J_{-1}} \sum_{j=0}^{\infty} \frac{J_j B_j \tilde{\Pi}_j^{(\alpha)}}{\Pi_j^{(\gamma)}} \tag{C11}$$

and

$$a_{\tilde{k}+1} = -\frac{1}{J_{-1}} \left(K_{\tilde{k}+1} \sum_{j=\tilde{k}+1}^{\infty} \frac{J_j B_j \Pi_j^{(\alpha)}}{\Pi_j^{(\gamma)}} + J_{\tilde{k}+1} \sum_{j=0}^{\tilde{k}} \frac{\Theta_j K_j B_j \Pi_j^{(\alpha)}}{\Pi_j^{(\gamma)}} \right). \tag{C12}$$

The factors Θ_j assume different values, depending on λ:

$$\lambda < 0\colon\ \Theta_j = 1,$$
$$\lambda = 0\colon\ \Theta_j = \gamma_{k^*}$$
$$\lambda > 0\colon\ \Theta_j = \begin{cases} \gamma_{k^*}\gamma_{\hat{k}} & \text{for } j < \hat{k} \\ \gamma_{k^*} & \text{for } \hat{k} \le j < k^* \\ 1 & \text{for } k^* \le j \le \tilde{k} \end{cases}$$

Note that in these expression no divisions by γ_{k^*} and $\gamma_{\hat{k}}$ occur and hence both coefficients a_0 as well as $a_{\tilde{k}+1}$ assume well defined values in the limit $s \to \lfloor s \rceil$. We finish this section by noticing that, for $|\lambda| = 2$, there are specific s values for which this construction fails since J_{-1} vanishes. Similar to the discussion in Sec. IV D 2 [see, in particular, Eq. (90)], we conclude that these values have to be considered as QNMs to be treated in Appendix D.

APPENDIX D: ALGEBRAICALLY SPECIAL QNMS

a. Polynomial solutions to the homogeneous Laplace transformed equation

For gravitational perturbations $|\lambda| = 2$, specific QNMs arise, the so-called algebraically special $s_{(\ell)}$ values which are negative integers. The characterization of QNMs in terms of the points (i) and (ii) in Sec. IV D 2 fails because (for each $s \in \mathbb{Z}^-$) the corresponding coefficients H_k and I_k cannot be defined for all k. However, it turns out that for $s = s_{(\ell)}$ a polynomial solution $\phi_{(\ell)}$ to the homogeneous problem (27) can be found. This means that the characterization of QNMs in terms of point (iii) in Sec. IV D 2 still holds and should therefore be regarded as a generically valid definition of QNMs for perturbations in the asymptotically flat Schwarzschild spacetime.

The solution $\phi_{(\ell)}$ emerges through the following considerations. Let us write $\phi_{(\ell)}$ as in (28) as Taylor expansion about $\sigma = 1$ with coefficients H_k that are *not* subject to the scaling condition in (31) but are normalized in the sequel through a different requirement. We look at the corresponding recurrence relation (29), denoted for the indexes $k \in \{j-1, j, j+1, j+2\}$:

$$\alpha_{j-1}H_j + \beta_{j-1}H_{j-1} + \gamma_{j-1}H_{j-2} = 0 \tag{D1}$$

$$\alpha_j H_{j+1} + \beta_j H_j + \gamma_j H_{j-1} = 0 \tag{D2}$$

$$\alpha_{j+1}H_{j+2} + \beta_{j+1}H_{j+1} + \gamma_{j+1}H_j = 0 \tag{D3}$$

$$\alpha_{j+2}H_{j+3} + \beta_{j+2}H_{j+2} + \gamma_{j+2}H_{j+1} = 0 \tag{D4}$$

It can be verified explicitly that for[19]

$$|\lambda| = 2, \qquad s = s_{(\ell)} = -\frac{1}{3}(\ell-1)\ell(\ell+1)(\ell+2), \qquad j = -s-2$$

the following properties arise:

(1) The coefficient γ_{-s} vanishes, $\gamma_{-s} = \gamma_{j+2} = 0$.
(2) The 2×2-matrix

$$\hat{M} = \begin{pmatrix} \beta_j & \alpha_j \\ \gamma_{j+1} & \beta_{j+1} \end{pmatrix}$$

is singular and possesses the nontrivial null eigenvector

$$\vec{v} = \begin{pmatrix} \ell^2+\ell-3 \\ 1-\lambda \end{pmatrix}$$

satisfying $\hat{M}\,\vec{v} = 0$.
(3) Additionally, we have for
(a) $\lambda = -2$ that $\alpha_{j-1} = 0$.
(b) $\lambda = +2$ that $\gamma_j = 0$.

Now, we may write (D2), (D3) in the form

$$\hat{M}\begin{pmatrix} H_j \\ H_{j+1} \end{pmatrix} = -\begin{pmatrix} \gamma_j H_{j-1} \\ \alpha_{j+1}H_{j+2} \end{pmatrix} \tag{D5}$$

The corresponding algebraically special solutions $\phi_{(\ell)}$ are characterized by the following properties:

(A) $H_k = 0$ for $k \ge j+2$.

[19] In [32], the algebraically special Laplace parameters are given by $\bar{s}_{(\ell)} = \frac{1}{2}s_{(\ell)}$, cf. (25).

(B) $H_k = 0$ for $k < 0$. With statement (A) we conclude that $\phi_{(\ell)}$ is a polynomial of order $\frac{1}{3}(\ell-1)\ell(\ell+1)(\ell+2)-1$.

(C) The coefficients (H_j, H_{j+1}) form a null eigenvector of $\hat{M}$, i.e.

$$\begin{pmatrix} H_j \\ H_{j+1} \end{pmatrix} = K\vec{v} = K\begin{pmatrix} \ell^2+\ell-3 \\ 1-\lambda \end{pmatrix} \tag{D6}$$

with some constant K.

The property (D6) means that (D5) is realized for the vanishing right-hand side; i.e., we have

$$\gamma_j H_{j-1} = 0 \tag{D7}$$

$$\alpha_{j+1} H_{j+2} = 0. \tag{D8}$$

Let us first look at (D8). As $\alpha_{j+1} = s_{(\ell)}\lambda \neq 0$ we have that $H_{j+2} = 0$. Looking now at (D4) it follows with $\gamma_{j+2} = 0$ (see point (1) above) and $\alpha_{j+2} = (\lambda-1)(s-1) \neq 0$ that $H_{j+3} = 0$. With the two vanishing coefficients $H_{j+2} = 0 = H_{j+3}$, the upwards recurrence relation

$$H_{k+1} = -\frac{1}{\alpha_k}(\beta_k H_k + \gamma_k H_{k-1}), \qquad k \geq j+3$$

tells us that all $H_k = 0$ for $k \geq j+2$; i.e., we obtain consistency with the above statement (A).

The first property (D7) is realized differently for the two cases $\lambda = -2$ and $\lambda = 2$. Let us start with the discussion of the situation $\lambda = -2$. As $\gamma_j = 4 - 2\lambda = 8 \neq 0$, we have $H_{j-1} = 0$. With the property 3.(a) above and $\gamma_{j-1} = 9 - 3\lambda = 15 \neq 0$, we obtain from (D1) that $H_{j-2} = 0$. Now, with $H_{j-1} = 0 = H_{j-2}$, the downwards recurrence relation

$$H_{k-1} = -\frac{1}{\gamma_k}(\alpha_k H_{k+1} + \beta_k H_k), \qquad k \leq j-2$$

tells us that all $H_k = 0$ for $k \leq j-1$, thus realizing in particular the above statement (B). Taking (D6) into account, the algebraically special polynomial solution amounts thus to

$$\phi_{(\ell)} = K(1-\sigma)^j[(\ell^2+\ell-3) + 3(1-\sigma)]$$

for

$$\lambda = -2, \qquad s = s_{(\ell)}, \qquad j = -s_{(\ell)} - 2.$$

For the remaining case $\lambda = 2$, we have $\gamma_j = 0$ [cf. point (3)(b)] and, hence, (D7) is realized trivially. Let us now look at the recurrence relation for the indexes $k = 0, \ldots, j-1$, where we assume that $H_{-1} = 0$ in order to satisfy the above statement (B), i.e.

$$\begin{aligned} \alpha_0 H_1 + \beta_0 H_0 &= 0 \\ \alpha_1 H_2 + \beta_1 H_1 + \gamma_1 H_0 &= 0 \\ &\vdots \\ \alpha_{j-2} H_{j-1} + \beta_{j-2} H_{j-2} + \gamma_{j-2} H_{j-3} &= 0 \\ \beta_{j-1} H_{j-1} + \gamma_{j-1} H_{j-2} &= -\alpha_{j-1} H_j \\ &= -K\alpha_{j-1}(\ell^2+\ell-3). \end{aligned} \tag{D9}$$

Here we have rewritten the very last relation for $k = j-1$ such that the quantity H_j known from (D6) appears as inhomogeneity on the right-hand side. Now, (D9) forms a system of j linear equations to determine uniquely the coefficients $\{H_0, \ldots, H_{j-1}\}$, thereby realizing $H_{-1} = 0$ through which the solution becomes analytic at $\sigma = 1$. We thus obtain for

$$\lambda = 2, \qquad s = s_{(\ell)}, \qquad j = -s_{(\ell)} - 2$$

the algebraically special polynomial solution as

$$\phi_{(\ell)} = \sum_{k=0}^{j+1} H_k (1-\sigma)^k$$

with the coefficients $\{H_0, \ldots, H_{j-1}\}$ fixed by (D9) and $\{H_j, H_{j+1}\}$ given through (D6). In the following, we use polynomial solutions $\phi_{(\ell)}$ which are normalized by the requirement $K = 1$. Note that the scaling in (31) would not work in the case $\lambda = -2$.

b. Algebraically special QNM amplitudes

A characterization that works well for the entirety of QNMs is given by the condition $J_{-1} = 0$ with J_k introduced in (C3) [see also (42)]. Clearly, then the computation of a_0 and $a_{\tilde{k}+1}$ according to (C11) and (C12) will fail, which leads us to the conclusion that in the vicinity of the algebraically special QNM $s_{(\ell)}$ the Laplace transform $\hat{V}$ is of the form (120), i.e. it possesses a single pole there. As $s_{(\ell)}$ is located on the branch cut, we need to consider separately the approach $s \to s_{(\ell)}$ from above ($\arg(s) \to \pi$) and from below ($\arg(s) \to -\pi$), i.e. $s \to s^{\pm}_{(\ell)}$. Alternatively, $\hat{V}$ can be regarded as being defined on multiple sheets in the complex s plane where the negative s axis presents the transition between the sheets. At the two s values $s = s^{\pm}_{(\ell)}$, the Laplace transform $\hat{V}$ possesses single poles with residues $\eta^{\pm}_{(\ell)}\phi_{(\ell)}$, which by virtue of (11) satisfy $\eta^{-}_{(\ell)} = [\eta^{+}_{(\ell)}]^*$. Considering the representation (15) of the

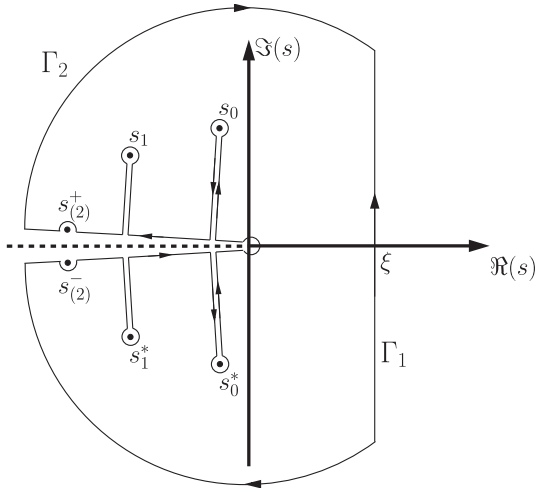

FIG. 14. Deformed integration path Γ_2 for the inverse Laplace transformation in the case $|\lambda| = 2$ where algebraically special QNMs $s^{\pm}_{(\ell)} \in \mathbb{R}^-$ are present. The Laplace transform $\hat{V}$ is defined on multiple sheets where the negative s axis presents the transition between the sheets. At $s = s^{\pm}_{(\ell)}$, $\hat{V}$ possesses single poles with residues $\eta^{\pm}_{(\ell)}\phi_{(\ell)}$, and the integration is to be performed along corresponding infinitesimal semicircles about $s^{\pm}_{(\ell)}$.

wave field V which we now evaluate along the deformed integration path Γ_2 displayed in Fig. 14, we find that in the limit of infinitesimal semicircles about the algebraically special QNMs $s^{\pm}_{(\ell)}$ the contributions

$$\frac{1}{2\pi i}\cdot \pi i \mathrm{Res}_{s^{\pm}_{(\ell)}}(\hat{V}e^{\tau s_{(\ell)}}),$$

arise, i.e. in sum:

$$\frac{1}{2}(\eta^-_{(\ell)}\phi_{(\ell)}e^{\tau s_{(\ell)}} + \eta^+_{(\ell)}\phi_{(\ell)}e^{\tau s_{(\ell)}}) = \Re(\eta^+_{(\ell)})\phi_{(\ell)}e^{\tau s_{(\ell)}}.$$

Thus, the corresponding spectral decomposition (see Sec. V) of the wave field satisfying the dissipative wave equation (9) assumes the form:

$$V(\tau,\sigma) = 2\sum_{n=0}^{\infty}\Re(\eta_n\phi_n(\sigma)e^{\tau s_n}) + \Re(\eta^+_{(\ell)})\phi_{(\ell)}(\sigma)e^{\tau s_{(\ell)}} + \int_{-\infty}^{0}\eta(s)\phi(\sigma;s)e^{\tau s}ds, \tag{D10}$$

where the set $\{s_n\}_{n=0}^{\infty}$ contains only those quasinormal modes for which $\Im(s_n) > 0$.

In order to determine the amplitude $\eta^+_{(\ell)}$, we proceed along the same line of reasoning as in Sec. IV E. In particular, the analogue of Eq. (104) for negative integer s values can be derived by means of Eq. (C11), with the source coefficient B_k being replaced by $(B_k - \eta^+_{(\ell)}C_k)$ where C_k is given by (105) [see also (100)] with the Taylor coefficients H_k of $\phi_{(\ell)}$. Requiring the regularity of the corresponding coefficient $g^+_0(s_{(\ell)})$, we obtain

$$\eta^+_{(\ell)} = \frac{\sum_{k=0}^{\infty}J^+_k B_k \frac{\tilde{\Pi}^{(\alpha)}_k}{\Pi^{(\gamma)}_k}}{\sum_{k=0}^{\infty}J^+_k C_k \frac{\tilde{\Pi}^{(\alpha)}_k}{\Pi^{(\gamma)}_k}} \quad \text{for } \lambda = +2. \tag{D11}$$

We emphasize, however, that this procedure works only for $\lambda = +2$. For $\lambda = -2$, we observe that $\tilde{\Pi}^{(\alpha)}_k = 0$ for $k > \lambda - s$ and $J^+_k = 0$ for $k \le \lambda - s$. Hence, every addend of the sum in (C11) vanishes, regardless of the source coefficient B_k. This means that this equation cannot be used to establish the amplitude $\eta^+_{(\ell)}$. Instead, the corresponding formula (C12) can be employed. Requiring a regular coefficient $g^+_{\tilde{k}+1}(s_{(\ell)})$ we find

$$\eta^+_{(\ell)} = \frac{K_{\tilde{k}+1}\sum_{k=\tilde{k}+1}^{\infty}J^+_k B_k \frac{\Pi^{(\alpha)}_k}{\Pi^{(\gamma)}_k} + J^+_{\tilde{k}+1}\sum_{k=0}^{\tilde{k}}K_k B_k \frac{\Pi^{(\alpha)}_k}{\Pi^{(\gamma)}_k}}{K_{\tilde{k}+1}\sum_{k=\tilde{k}+1}^{\infty}J^+_k C_k \frac{\Pi^{(\alpha)}_k}{\Pi^{(\gamma)}_k} + J^+_{\tilde{k}+1}\sum_{k=0}^{\tilde{k}}K_k C_k \frac{\Pi^{(\alpha)}_k}{\Pi^{(\gamma)}_k}} \tag{D12}$$

for $\lambda = -2$.

[1] T. Regge and J. Wheeler, Phys. Rev. **108**, 1063 (1957).
[2] F. J. Zerilli, Phys. Rev. Lett. **24**, 737 (1970).
[3] F. J. Zerilli, Phys. Rev. D **2**, 2141 (1970).
[4] W. P. J. M. Bardeen, J. Math. Phys. (N.Y.) **14**, 7 (1973).
[5] E. T. Newman and R. Penrose, J. Math. Phys. (N.Y.) **3**, 566 (1962); **4**, 998(E) (1963).
[6] S. A. Teukolsky, Astrophys. J. **185**, 635 (1973).
[7] C. V. Vishveshwara, Nature (London) **227**, 936 (1970).
[8] B. P. A. *et al.* (LIGO Scientific), Phys. Rev. Lett. **116**, 061102 (2016).
[9] V. Cardoso, E. Franzin, and P. Pani, Phys. Rev. Lett. **116**, 171101 (2016).
[10] C. Chirenti and L. Rezzolla, arXiv:1602.08759.
[11] R. Price, Phys. Rev. D **5**, 2419 (1972).
[12] S. Chandrasekhar, *The Mathematical Theory of Black Holes*, (Oxford University Press, New York, 1983).

[13] K. D. Kokkotas and B. G. Schmidt, Living Rev. Relativ. **2**, 2 (1999).
[14] H.-P. Nollert, Classical Quantum Gravity **16**, R159 (1999).
[15] E. Berti, V. Cardoso, and A. O. Starinets, Classical Quantum Gravity **26**, 163001 (2009).
[16] E. Leaver, Proc. R. Soc. A **402**, 285 (1985).
[17] E. W. Leaver, J. Math. Phys. (N.Y.) **27**, 1238 (1986).
[18] E. W. Leaver, Phys. Rev. D **34**, 384 (1986).
[19] V. Cardoso, Ph.D. thesis, Instituto Superior Técnico, Lisbon, 2003.
[20] A. Bachelot and A. Motet-Bachelot, Annales de l'I.H.P. Physique théorique **59**, 3 (1993).
[21] N.-P. Nollert and R. Price, J. Math. Phys. (N.Y.) **40**, 980 (1999).
[22] Y. Sun and R. H. Price, Phys. Rev. D **38**, 1040 (1988).
[23] N. Andersson, Phys. Rev. D **51**, 353 (1995).
[24] E. Berti and V. Cardoso, Phys. Rev. D **74**, 104020 (2006).
[25] F. Finster, N. Kamran, J. Smoller, and S.-T. Yau, Adv. Theor. Math. Phys. **7**, 25 (2003).
[26] F. Finster, N. Kamran, J. Smoller, and S.-T. Yau, Commun. Math. Phys. **230**, 201 (2002).
[27] F. Finster, N. Kamran, J. Smoller, and S.-T. Yau, Commun. Math. Phys. **260**, 257 (2005).
[28] F. Finster, N. Kamran, J. Smoller, and S.-T. Yau, Commun. Math. Phys. **264**, 465 (2006).
[29] F. Finster and J. Smoller, Adv. Theor. Math. Phys. **13**, 71 (2009).
[30] A. Zenginoglu, Phys. Rev. D **83**, 127502 (2011).
[31] J. Frauendiener, Living Rev. Relativ. **7**, 1 (2004).
[32] S. Chandrasekhar, Proc. Roy. Soc. A **392**, 1 (1984).
[33] D. Schinkel, R. P. Macedo, and M. Ansorg, Classical Quantum Gravity **31**, 165001 (2014).
[34] R. P. Macedo and M. Ansorg, J. Comput. Phys. **276**, 357 (2014).
[35] J. N. Goldberg, A. J. MacFarlane, E. T. Newman, F. Rohrlich, and E. C. G. Sudarshan, J. Math. Phys. (N.Y.) **8**, 2155 (1967).
[36] V. Cardoso, https://centra.tecnico.ulisboa.pt/~vitor/.
[37] I. S. Gradshteyn and I. M. Ryzhik, *Table of Integrals, Series, and Products*, 7th ed. (Elsevier, New York, 2007).
[38] P. D. Lax and R. S. Phillips, Bull. Am. Math. Soc. **70**, 130 (1967).
[39] E. Harms, S. Bernuzzi, and B. Bruegmann, Classical Quantum Gravity **30**, 115013 (2013).